NASA/TM—2009-215613 AIAA–2008–4919

NEXT Long-Duration Test Plume and Wear Characteristics After 16,550 h of Operation and 337 kg of Xenon Processed

Daniel A. Herman
ASRC Aerospace Corporation, Cleveland, Ohio

George C. Soulas and Michael J. Patterson
Glenn Research Center, Cleveland, Ohio

May 2009

NASA STI Program . . . in Profile

Since its founding, NASA has been dedicated to the advancement of aeronautics and space science. The NASA Scientific and Technical Information (STI) program plays a key part in helping NASA maintain this important role.

The NASA STI Program operates under the auspices of the Agency Chief Information Officer. It collects, organizes, provides for archiving, and disseminates NASA's STI. The NASA STI program provides access to the NASA Aeronautics and Space Database and its public interface, the NASA Technical Reports Server, thus providing one of the largest collections of aeronautical and space science STI in the world. Results are published in both non-NASA channels and by NASA in the NASA STI Report Series, which includes the following report types:

- TECHNICAL PUBLICATION. Reports of completed research or a major significant phase of research that present the results of NASA programs and include extensive data or theoretical analysis. Includes compilations of significant scientific and technical data and information deemed to be of continuing reference value. NASA counterpart of peer-reviewed formal professional papers but has less stringent limitations on manuscript length and extent of graphic presentations.

- TECHNICAL MEMORANDUM. Scientific and technical findings that are preliminary or of specialized interest, e.g., quick release reports, working papers, and bibliographies that contain minimal annotation. Does not contain extensive analysis.

- CONTRACTOR REPORT. Scientific and technical findings by NASA-sponsored contractors and grantees.

- CONFERENCE PUBLICATION. Collected papers from scientific and technical conferences, symposia, seminars, or other meetings sponsored or cosponsored by NASA.

- SPECIAL PUBLICATION. Scientific, technical, or historical information from NASA programs, projects, and missions, often concerned with subjects having substantial public interest.

- TECHNICAL TRANSLATION. English-language translations of foreign scientific and technical material pertinent to NASA's mission.

Specialized services also include creating custom thesauri, building customized databases, organizing and publishing research results.

For more information about the NASA STI program, see the following:

- Access the NASA STI program home page at *http://www.sti.nasa.gov*

- E-mail your question via the Internet to *help@sti.nasa.gov*

- Fax your question to the NASA STI Help Desk at 301–621–0134

- Telephone the NASA STI Help Desk at 301–621–0390

- Write to:
  NASA Center for AeroSpace Information (CASI)
  7115 Standard Drive
  Hanover, MD 21076–1320

NASA/TM—2009-215613 AIAA–2008–4919

NEXT Long-Duration Test Plume and Wear Characteristics After 16,550 h of Operation and 337 kg of Xenon Processed

Daniel A. Herman
ASRC Aerospace Corporation, Cleveland, Ohio

George C. Soulas and Michael J. Patterson
Glenn Research Center, Cleveland, Ohio

Prepared for the
44th Joint Propulsion Conference and Exhibit
cosponsored by the AIAA, ASME, SAE, and ASEE
Hartford, Connecticut, July 21–23, 2008

National Aeronautics and
Space Administration

Glenn Research Center
Cleveland, Ohio 44135

May 2009

This report contains preliminary findings,
subject to revision as analysis proceeds.

Level of Review: This material has been technically reviewed by technical management.

Available from

NASA Center for Aerospace Information
7115 Standard Drive
Hanover, MD 21076–1320

National Technical Information Service
5285 Port Royal Road
Springfield, VA 22161

Available electronically at http://gltrs.grc.nasa.gov

NEXT Long-Duration Test Plume and Wear Characteristics After 16,550 h of Operation and 337 kg of Xenon Processed

Daniel A. Herman
ASRC Aerospace Corporation
Cleveland, Ohio 44135

George C. Soulas and Michael J. Patterson
National Aeronautics and Space Administration
Glenn Research Center
Cleveland, Ohio 44135

Abstract

The NASA's Evolutionary Xenon Thruster (NEXT) program is developing the next-generation ion propulsion system with significant enhancements beyond the state-of-the-art. The NEXT ion propulsion system provides improved mission capabilities for future NASA science missions to enhance and enable Discovery, New Frontiers, and Flagship-type NASA missions. As part of a comprehensive thruster service life assessment utilizing both testing and analyses, a Long-Duration Test (LDT) was initiated to validate and qualify the NEXT propellant throughput capability to a qualification-level of 450 kg, 1.5 times the mission-derived throughput requirement of 300 kg. This wear test is being conducted with a modified, flight-representative NEXT engineering model ion thruster, designated EM3. As of June 25, 2008, the thruster has accumulated 16,550 h of operation: the first 13,042 h at the thruster full-input-power of 6.9 kW with 3.52 A beam current and 1800 V beam power supply voltage. Operation since 13,042 h, i.e., the most recent 3,508 h, has been at an input power of 4.7 kW with 3.52 A beam current and 1180 V beam power supply voltage. The thruster has processed 337 kg of xenon (Xe) surpassing the NSTAR propellant throughput demonstrated during the extended life testing of the Deep Space 1 flight spare. The NEXT LDT has demonstrated a total impulse of 13.3×10^6 N·s; the highest total impulse ever demonstrated by an ion thruster. Thruster plume diagnostics and erosion measurements are obtained periodically over the entire NEXT throttle table with input power ranging 0.5 to 6.9 kW. Observed thruster component erosion rates are consistent with predictions and the thruster service life assessment. There have not been any observed anomalous erosion and all erosion estimates indicate a thruster throughput capability that exceeds ~750 kg of Xe, an equivalent of 36,500 h of continuous operation at the full-power operating condition. This paper presents the erosion measurements and plume diagnostic results for the NEXT LDT to date with emphasis on the change in thruster operating condition and resulting impact on wear characteristics. Ion optics' grid-gap data, both cold and operating, are presented. Performance and wear predictions for the LDT throttle profile are presented.

Nomenclature

BOL	beginning-of-life
CRA	accelerator grid center-radius aperture
DCA	discharge cathode assembly
DCIU	digital control interface unit
DS1	Deep Space 1
ELT	Extended Life Test
EM	engineering model
EPT	electric propulsion thruster
GRC	NASA Glenn Research Center
HiPEP	High Power Electric Propulsion

Isp	specific impulse, s
J_B	beam current, A
J_{DC}	discharge current, A
J_{NK}	neutralizer keeper current, A
LDT	Long-Duration Test
m_C	discharge cathode flowrate, sccm
m_M	main plenum flowrate, sccm
m_N	neutralizer cathode flowrate, sccm
NCA	neutralizer cathode assembly
NEXT	NASA's Evolutionary Xenon Thruster
NSTAR	NASA Solar Electric Propulsion Technology Applications Readiness
ORA	outer-radius apertures
P_{IN}	thruster input power, kW
PM	prototype model
PMS	propellant management system
PPU	power processing unit
QCM	quartz-crystal microbalance
RGA	residual gas analyzer
SEP	Solar Electric Propulsion
T	Thrust, *mN*
V_A	accelerator grid voltage, V
V_B	beam power supply voltage, V
V_{DC}	discharge voltage, V
VF–16	Vacuum Facility 16
WT	wear test
Xe	xenon
ϕ	diameter

Introduction

The success of the Deep Space 1 (DS1) mission, utilizing the NASA Solar Electric Propulsion Technology Applications Readiness (NSTAR) ion propulsion system, has secured the future of electric propulsion technology application in achieving and enhancing NASA's solar system exploration objectives in the 21st century (Refs. 1 to 4). In 2002, NASA Glenn Research Center (GRC) was selected to lead the development of NASA's Evolutionary Xenon Thruster (NEXT) under the Next Generation Ion project. The GRC-led NEXT team includes as partners the Jet Propulsion Laboratory, Aerojet—Redmond Operations, and L3 Electron Technologies (formerly Boeing Electron Dynamic Devices). The NEXT project is tasked with development of the next-generation ion propulsion system. The NEXT Solar Electric Propulsion (SEP) system design enhances and enables Discovery, New Frontiers, and other exploration mission classes, including Mars sample return (Refs. 5 and 6). The NEXT propulsion system is significantly more advanced than current state-of-the-art, NSTAR, ion thrusters and consists of a high-performance, 7-kW electric propulsion thruster (EPT); a lightweight, high-efficiency power processing unit (PPU); an advanced propellant management system (PMS); a lightweight thruster gimbal; and key elements of a digital control interface unit (DCIU) including software algorithms (Refs. 7 and 8).

The NEXT system development Phase I effort, successfully completed in August 2003, included: building multiple engineering model (EM) thrusters; characterizing EM thruster performance; conducting a 2,000 h wear test (WT); developing a breadboard PMS, a breadboard PPU, and a single-string DCIU simulator; and a breadboard system integration test of the entire NEXT system (Refs. 9 to 11). After demonstrating component and system technology at a breadboard level, the NEXT Phase II activities include: the development of flight-like engineering model components; performance, environmental, and integration testing; and thruster life assessment through both analysis and testing to validate the

technology approach and hardware design (Ref. 12). The hardware development activities for Phase II, initiated in October 2003, include: prototype model (PM) thruster design, an EM PMS design, an EM PPU design, and a breadboard gimbal design (Refs. 13 to 16).

The NEXT Phase II thruster effort, led by Aerojet, includes the design, development, manufacturing, and delivery of up to two PM NEXT thrusters for performance characterization, environmental qualification, and integration testing. The NEXT LDT test article has been modified to a flight-representative configuration so it is more comparative to the NEXT PM thruster by incorporating PM ion optics and a graphite discharge cathode keeper electrode.

Validation of the NEXT thruster service life capability is being addressed via a comprehensive service life validation scheme utilizing a combination of test and analyses. A NEXT service life assessment was conducted at GRC employing several models to evaluate all known failure modes incorporating the results of the NEXT 2,000 h WT conducted on a NEXT EM ion thruster at 6.9 kW input power (Refs. 17 and 18). The assessment predicts the earliest failure occurring sometime after 750 kg of Xe throughput, well beyond the mission-derived propellant throughput requirement of 300 kg (Ref. 18). To validate the NEXT thruster service life model and qualify the NEXT thruster, the NEXT Long-Duration Test (LDT) was initiated. The purpose of the NEXT LDT is to: 1) characterize thruster performance over the test duration, 2) measure the erosion rates of critical thruster components, 3) identify unknown life-limiting mechanisms, and 4) demonstrate 1.5 times the mission-derived propellant throughput requirement resulting in a qualification propellant throughput requirement of at least 450 kg. In addition to the NEXT LDT, multiple component-level lifetime tests are underway or planned for the NEXT program to augment the results of the LDT (Ref. 19). The NEXT thruster service life analysis is being updated based upon the LDT data and component testing findings as well as being applied for potential mission opportunities to assess thruster wear and performance (Ref. 20).

The thruster operation has been carried out in a multi-phase approach: phase 1) quick sprint at full power to verify extended duration functionality and validate end-of-life prediction, phase 2) thruster operation in a throttled mission-representative profile that focuses on operating points of interest with regard to wear characteristics and life-limiting phenomena, phase 3) operation to failure at the thruster operating point with the shortest lifetime, i.e., full-input power. Phase 1 operation has been completed demonstrating 13,042 h of operation at the full-input-power with performance and erosion characteristics supporting the thruster lifetime throughput capability predicted by the NEXT service life assessment of ~750 kg. Phase two operation has begun and to date 3,508 h of operation at 4.7 kW input power has been demonstrated.

Test Article

The Next Generation Ion solicitation, acknowledging that future exploration and inner solar system sample return missions will demand increased power range, throttle-ability, performance, and throughput at reduced specific mass, established a set of challenging mission requirements for the next generation of ion thrusters. The NEXT thruster inherits the knowledge gained through the NSTAR thruster development and flight experience, while significantly increasing the maximum thruster power level and improving key thruster performance parameters. The NEXT LDT is being conducted with an EM ion thruster, designated EM3, shown in Figure 1. The EM3 thruster has been modified to a flight-representative configuration so it is more comparative to the NEXT PM thruster by incorporating PM ion optics and a graphite discharge cathode keeper electrode. To reduce the risk of a facility-induced failure of the thruster, the neutralizer assembly was enclosed to protect insulators from sputter deposition and all critical surfaces were grit-blasting for flake retention. The PM ion optics beam extraction diameter was reduced from the 40 cm diameter of the EM thrusters to 36 cm diameter to reduce outer-radius accelerator aperture erosion caused by beamlet over-focusing in these low current density regions (Refs. 17, 21, and 22). Reducing the ion optics beam extraction diameter from 40 cm also reduces the maximum thruster beam divergence and neutral loss rate without a significant increase in discharge losses (Ref. 23). The PM ion optics geometry retains many of the key features of the EM design, however, improved manufacturing

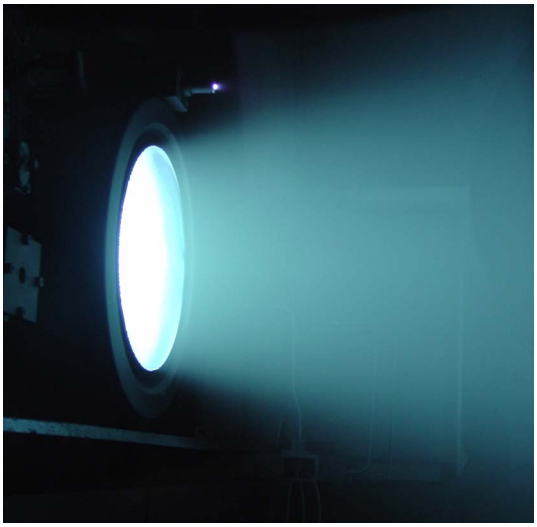

Figure 1.—NEXT EM3 operating at full-power during the LDT.

techniques implemented by a new vendor led to: better control of aperture variation as a function of grid radius, a reduced and more consistent cusp profile, and elimination of "worm track" surface problems previously encountered (Ref. 24). The aperture variation for the PM accelerator grid is +1/–6 percent compared to +11/–16 percent for EM optics(Ref. 24). The PM ion optics mounting scheme has been altered to eliminate the buildup and relaxation of assembly and thermally-induced stresses that lead to the decreasing ion optics' grid-gap with test duration (Refs. 17, 25, and 26).

One of the unexpected findings from the NSTAR Extended Life Test (ELT) was the anomalous discharge cathode keeper erosion, which was more severe and qualitatively different than prior 1,000 h and 8,200 h NSTAR wear tests (Refs. 25, 27, and 28). Due to the complete NSTAR ELT discharge cathode keeper faceplate erosion and the NEXT EM 2,000 h wear test results, a graphite discharge cathode keeper is employed on EM3, similar to the NEXT PM thruster design, to mitigate keeper erosion. The erosion rate of carbon due to the low-energy discharge plasma ion impacts is over 20 times lower than molybdenum (Ref. 29), thus utilization of a graphite keeper electrode dramatically extends thruster service life.

The NEXT thruster, shown operating in Figure 1, is nominally a 0.5 to 6.9 kW input power Xe ion thruster with 2-grid ion optics with screen (+) upstream and accelerator (–) downstream electrodes. The technical approach for the NEXT design is a continuation of the derating philosophy used for the NSTAR ion thruster. A beam extraction area 1.6 times NSTAR allows higher thruster input power while maintaining low voltages and ion current densities, thus maintaining thruster longevity. The semi-conic discharge chamber utilizes a hollow cathode emitter with a ring-cusp magnetic topology created by high-strength, rare earth magnets for electron confinement. A flake retention scheme identical to that employed on the NSTAR thruster enhances the adhesion of thin films to the discharge chamber surfaces (Ref. 30). New, compact propellant isolators with higher voltage isolation capability than those used by the NSTAR thruster are utilized. The NEXT neutralizer design is mechanically similar to the International Space Station Plasma Contactor leveraging this extensive database to reduce risk. Additional description of the NEXT EM3 thruster design can be found in References 7, 31 to 34.

Test Support Hardware

The following section briefly describes the NEXT LDT supporting hardware. More detailed descriptions can be found in References 17, 34 to 36.

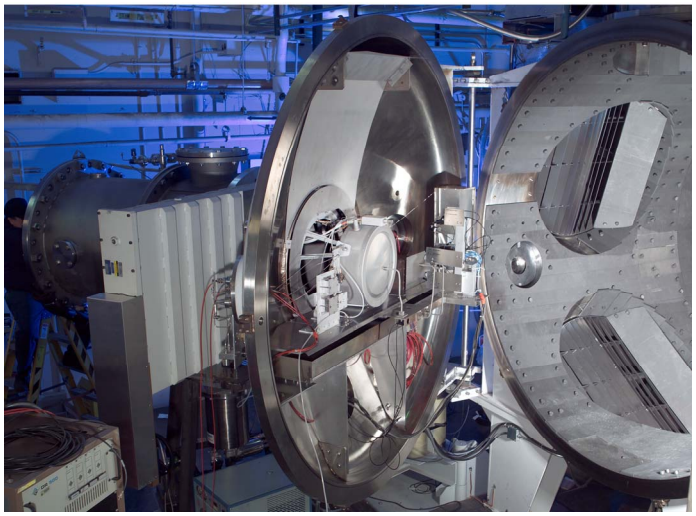

Figure 2.—VF–16 at GRC—end-cap opened. EM3 extends out the emergency bell jar in testing configuration.

Vacuum Facility and Facility Diagnostics

The NEXT LDT is being conducted in the 2.7 m diameter by 8.5 m long Vacuum Facility 16 (VF–16) at GRC, shown in Figure 2. VF–16 has an emergency bell jar on the end cap into which the thruster can be withdrawn and isolated in the event of a facility emergency. VF–16 is equipped with 10 cryogenic pumps for nominal thruster operation and an additional cryo-pump on the isolated bell jar for emergency use. With all 10 cryo-pumps operating, the base pressure is less than 3×10^{-7} torr. Facility pressure is monitored by two ionization gauges, a glass-tube ion gauge located on the facility wall 0.5 m downstream of the thruster and a dual-filament nude near-thruster ion gauge mounted 0.5 m radially beside EM3. In addition, the isolated bell jar has an ion gauge that is turned off during normal operation. The measured facility pumping speed, corrected for Xe, is 180 kL/s using the wall-mounted ion gauge. With 10 operational cryo-pumps, the near-thruster background pressure is 2.5×10^{-6} torr, corrected for Xe, when the thruster is operating at full-power. A quadrupole residual gas analyzer (RGA) measures and records the quantity of individual gas species inside VF–16 continuously every minute. All interior surfaces downstream of the thruster are lined with 1.2 cm thick graphite paneling to reduce the back-sputtered material flux to the thruster and test support hardware. The back-sputter rate, nominally 3 μm/khr when the thruster is at full-power, is monitored by a quartz-crystal microbalance (QCM) located next to the ion thruster. Three pinhole cameras are mounted next to the QCM and will be microscopically analyzed at the conclusion of the life test to determine the source of back-sputtered material. In addition to the pinhole cameras, five quartz witness plates are mounted along the length of the vacuum chamber wall.

Power Console and Xenon Feed System

A power console consisting of commercially available power supplies, similar to that described in Reference 37, powers the ion engine. A high-purity gas feed system provides Xe to the discharge cathode, discharge chamber main plenum, and neutralizer cathode through separate mass flow controllers. Xenon can be supplied to the discharge chamber main plenum by either a mass flow controller or an engineering model propellant management system kernel provided by Aerojet.

Diagnostics

A computerized data acquisition and control system is used to monitor and record ion engine and facility operations. A set of data consists of individual mass flow rates, ion engine currents measured with current shunts, voltages measured with voltage dividers, facility pressures, and the QCM measurement. Ion beam diagnostics include three staggered planar probes mounted onto a translation stage to measure radial ion current density profiles and an ExB probe, or Wien Filter, to measure the doubly-to-singly charged ion signature. Each molybdenum Faraday probe has 1-cm^2 circular current-collection area and is biased –30 V relative to facility ground to repel electrons. Faraday probes are fixed at axial positions of 20, 173, and 238 mm downstream of the accelerator grid. The collected currents are measured through separate isolated shunt resistors. The ExB probe is positioned 7.6 m downstream of the thruster on centerline, yielding a doubly-to-singly charged ion signature in the far-field. The ExB probe design is described in Reference 10. The Faraday probes and ExB probe are protected from the high-energy ion beam by parking the probes outside the beam and behind a graphite shutter, respectively. The LDT ion beam diagnostics are described in detail in Reference 36.

Erosion of critical ion engine components is monitored by six in-situ CCD cameras, shown in Figure 3, which capture erosion patterns and wear rates throughout the life test. The cameras image: the downstream neutralizer keeper and cathode orifice plate, the discharge cathode keeper and cathode orifice plate, accelerator grid apertures at various radial locations from centerline, and the cold grid-gap of the thruster ion optics. The cameras are mounted to a single-axis positioning system that moves the cameras radially in front of the thruster.

Operating Conditions and Performance Tests

The NEXT ion thruster is designed for SEP applications that experience variation in power available as solar flux changes at various distances from the sun throughout the mission. Ion thruster input power is designed to be throttled from 0.5 to 6.9 kW to accommodate this variation in available power. The NEXT LDT consists of three operating phases: 1) operate at the full-power point until 267 kg propellant throughput has been demonstrated, 2) throttle to assess extended operation at operating conditions of

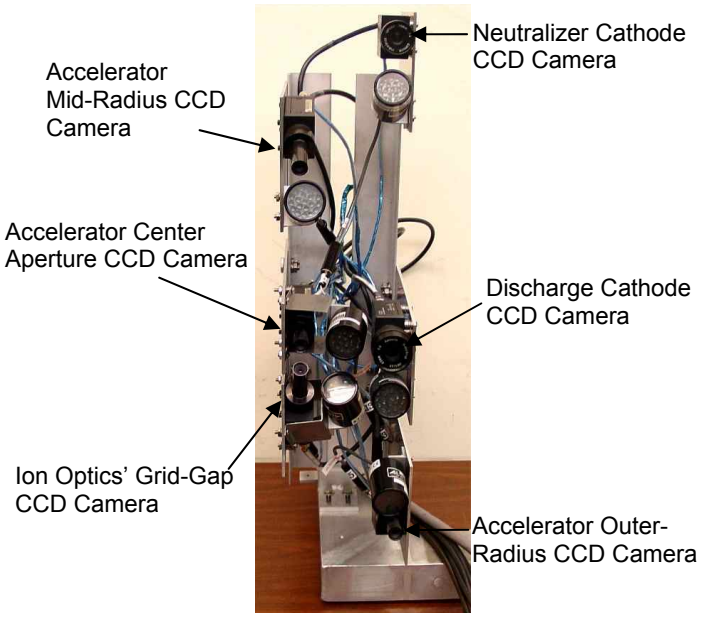

Figure 3.—Erosion cameras mounted to a vertical mast.

interest after 267 kg, and 3) throttle to full-power until either decision is made to end the test or the thruster fails. The LDT is currently in Phase 2 of thruster operations and has operated at full-power and the first throttled operating condition. The thruster full-input-power (6.9 kW) operating condition and first throttled operating condition (4.7 kW) are shown in Table 1. The input power indicated in Table 1 is a nominal operating power requirement from the NEXT throttle table at the thruster beginning-of-life and may differ slightly from thruster to thruster (Ref. 31).

TABLE 1.—NEXT LDT FULL-INPUT-POWER AND FIRST THROTTLED OPERATING CONDITIONS

P_{IN}, kW[a]	J_B, A	V_B, V	V_A, V	m_M, sccm	m_C, sccm	mN, sccm	J_{NK}, A
6.83	3.52	1800	–210	49.6	4.87	4.01	3.00
4.68	3.52	1180	–200	49.6	4.87	4.01	3.00

[a]Nominal value.

The proposed NEXT LDT throttling strategy is illustrated in Table 2 with operating durations subject to change if erosion or performance trends differ from projections. This throttling strategy demonstrates operation over the extremes of the NEXT throttling table including: highest power, highest total accelerating voltage, highest thermal load, condition with worst under-focusing at center-radius aperture location, condition with worst over-focusing at outer-radius locations, lowest power, lowest total accelerating voltage, lowest thermal load, and the condition with the highest ratio of discharge cathode emission to discharge cathode flow rate. Thruster performance is measured periodically over the entire throttle table regardless of thruster operating condition.

TABLE 2.—NEXT LDT PROPOSED THROTTLING STRATEGY

P_{IN}, kW[a]	J_B, A	V_B, V	Duration, kh	Segment throughput, kg	Segment total impulse, N·s
6.83	3.52	1800	13	267	1.11×10^{7}
4.68	3.52	1180	4	82	2.76×10^{6}
1.51	1.20	1020	2	19	5.80×10^{5}
6.83	3.52	1800	3	62	2.55×10^{6}
0.529	1.00	275	3	20	2.75×10^{5}
2.43	1.20	1800	2	15	5.78×10^{5}
		Totals	27	465	1.78×10^{7}

[a]Nominal value.

I. Thruster Performance

As of June 25, 2008, the NEXT EM3 thruster has accumulated 16,550 h of operation. The NEXT thruster has processed 337 kg of Xe illustrated in Figure 4; *surpassing the total propellant throughput processed by the DS1 flight spare in the NSTAR ELT (235 kg)*. The NEXT thruster has processed more than 4.5 times that of the DS1 NSTAR flight thruster. Figure 4 shows the NEXT LDT propellant throughput as a function of elapsed time with reference to the NSTAR ELT and flight DS1 thruster, the thruster throughput requirements from various mission analyses conducted using the NEXT propulsion system, and the NEXT qualification level throughput—450 kg (Refs. 26, 38, and 39). The NEXT thruster has demonstrated a total impulse of 13.3×10^{6} N·s to date; *the highest total impulse ever demonstrated by an ion thruster.* The NEXT milestone is also the highest total impulse ever demonstrated by an electric propulsion device with an input power less than 10 kW (Refs. 40). The NEXT LDT total impulse demonstrated exceeded that of the 30,000 h NSTAR ELT in less than one-third the thruster operating duration, shown in Figure 4.

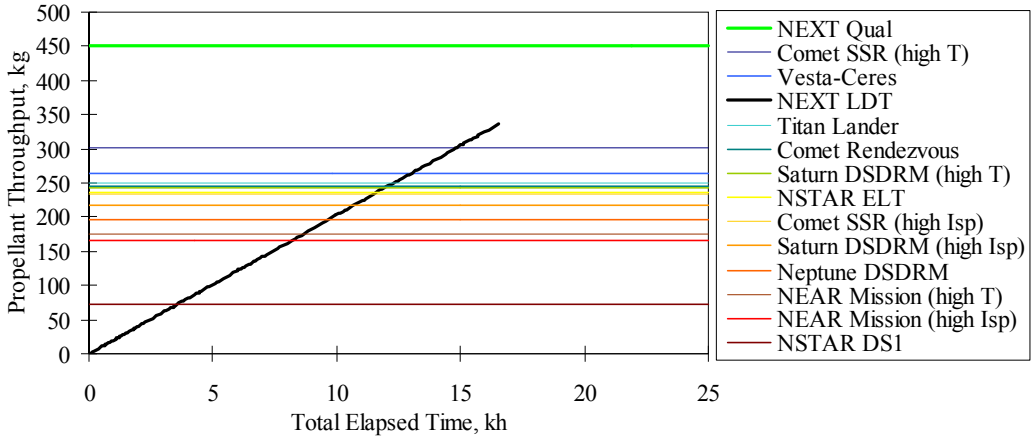

Figure 4.—NEXT LDT propellant throughput data as a function of time with reference milestones.

Performance of the thruster has been steady with minimal degradation. Erosion of critical thruster components has been within modeling predictions and consistent with the NEXT service life assessment (Refs. 20, 41, and 42). Several of the NSTAR ELT-observed wear anomalies have been significantly reduced and in most cases eliminated. There has been no observed discharge cathode keeper orifice erosion, no measured increase in accelerator grid aperture cusps except for the outer edge apertures, and no measured change in the cold grid-gap of the ion optics for the NEXT engine—all of which were observed during the NSTAR ELT of the DS1 flight spare (Ref. 26). NEXT LDT performance characteristics and thruster lifetime predictions are incorporated in References 20 and 43.

Beam Diagnostics and In-Situ Erosion Results

The plume diagnostics and erosion measurement results of the NEXT LDT are presented in this section. A number of high risk or life-limiting items were identified from the DS1 flight spare ELT. The results of the NSTAR ELT were considered and design changes made in the NEXT design to reduce or mitigate thruster failure modes and high risk items listed in Table 3.

TABLE 3.—NSTAR ELT THRUSTER HIGH RISK ITEMS, EROSION PHENOMENA, AND NEXT THRUSTER MITIGATION STRATEGIES

NSTAR ELT Issue	NEXT Mitigation Strategy	NEXT LDT Observations
Discharge cathode short (after 5850 h, 56 kg) and keeper faceplate completely eroded away exposing cathode.	Cathode keeper material changed to graphite to reduce sputter yield and erosion rate.	No keeper orifice diameter erosion observed. Substantial margin on keeper orifice plate erosion from 2,000 h wear test.[19]
Pit and groove erosion through the accelerator grid evident in post-test analysis.	Thicker accelerator grid to achieve longer life.	Groove erosion measurements indicate 700 to 800 kg propellant throughput before eroded through.
Ion optics cold grid-gap 30 percent decrease over test duration.	Redesigned ion optics mounting ring to better manage thermal stresses.	In-situ cold grid-gap measurement constant over test duration to date.
Electron backstreaming limit reached throttle value for full-power operation after ~10, 900 h (92 kg).	Thick accelerator grid optics utilized, highly focused beamlets at full-power reduce cusp erosion, and grid-gap decrease mitigated.	Electron backstreaming limit has been constant for all operating conditions over test duration. Negligible cusp erosion to date. Downstream erosion at steady-state.
Evidence of arc-tracking in low-voltage propellant isolator.	Low-voltage isolator eliminated. Isolation maintained by the high-voltage propellant isolator.	High impedance measured from anode to discharge cathode to date.

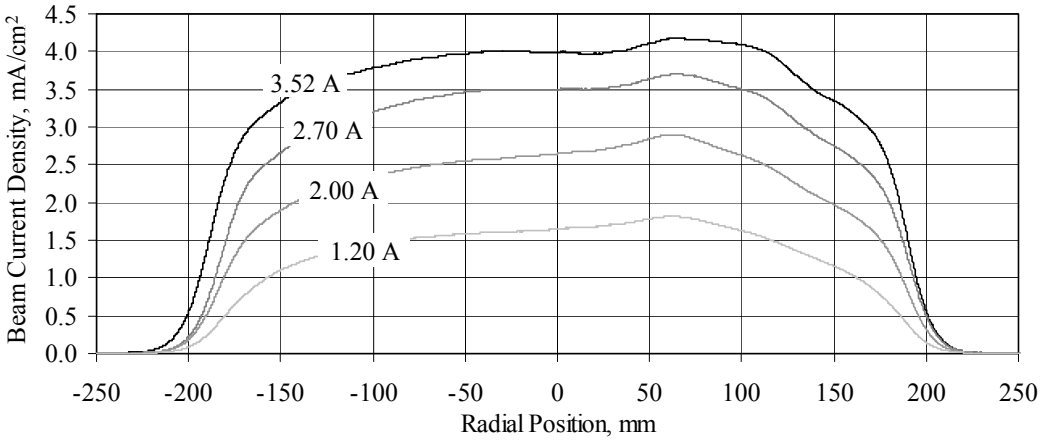

Figure 5.—Sample beam profiles for various beam currents at an axial position of 20 mm for V_B = 1800 V.

Radial Beam Current Density Profiles

Radial beam current density profiles are measured as close as 20 mm downstream from the geometric center of the ion optics. No attempt was made to repel charge-exchange ions from the probe nor account for secondary electron emission due to ion bombardment. Sample radial beam current density profiles at 20 mm axial position are plotted in Figure 5 for various beam currents demonstrating the shape functions of the ion current density profiles are similar at all beam currents evaluated. The radial profiles are also non-symmetric near centerline, which is an artifact of the engine discharge chamber plasma (Refs. 44 to 46).

Over the course of the LDT, the measured peak beam current density at full-power steadily increased with test duration, most notably for the closest probe. It is theorized that back-sputtered material accumulation on the probe and insulator between the probe and grounded guard has increased the probe collection area. Approximately 45 μm of carbon has been back-sputtered towards the thruster to date. Measurements of the back-sputter rate as a function of operating condition are consistent with pretest predictions indicating back-sputter rates of 3.0 and 1.7 μm/kh for the full-power and 4.7 kW operating conditions, respectively (Ref. 47). Multiple sweeps through the high-energy beam has been shown to remove this deposited material resulting in profiles consistent with the pretest profile. To remove the facility effect on beam profiles, only data taken with "clean" probes will be presepnted, i.e., after multiple sweeps obtained. Assuming azimuthal symmetry, integration of the radial beam current density profile at 20 mm axial location yields beam currents that are higher than the measured beam current by ~8 percent. Possible sources of error are discussed in References 44 and 45. This error is consistent with the 8 percent error observed during the NEXT 2,000 h WT (Ref. 35). The maximum beam current density has remained constant throughout the test duration, illustrated in Figure 6. The beam flatness parameter at full-power has also been constant when only "clean" probes are plotted in Figure 7. Comparison of the beam profiles at axial positions of 20 and 173 mm are shown in Figure 8 for t = 0 h and t = 13,300 h illustrating negligible change over the wear test duration. After 14,000 h of operation, while attempting to "clean" the Faraday probes, a short of the closest Faraday cup to the grounded shield developed and has prevented operation of this probe since. The remaining two downstream probes offer limited value because they have shown to be impacted by deposited material that cannot easily be cleaned off. The failure of the Faraday probe was one of the lessons learned from the NSTAR ELT that had been addressed by shielding the closest Faraday probe when in the stored position (Ref. 26). It is apparent that the shielding used in the NEXT LDT, which leaves a gap of several inches between the Faraday cup and the shield, is insufficient to prevent failure of this diagnostic.

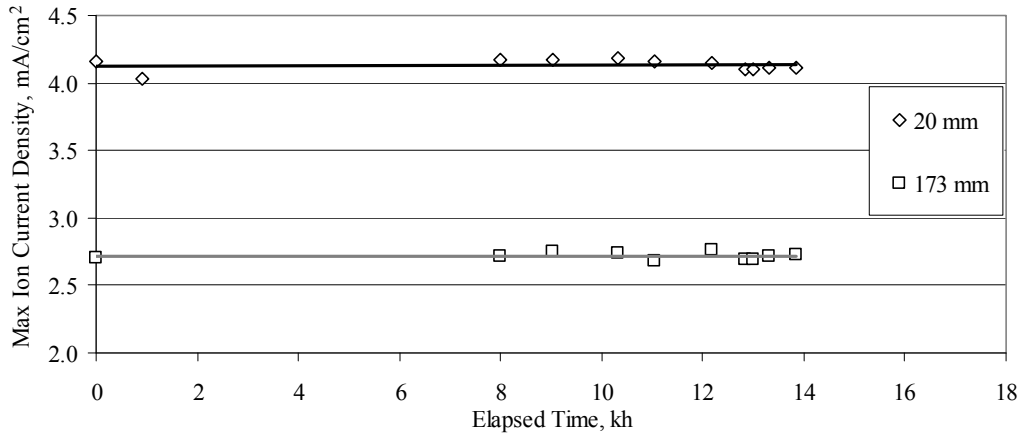

Figure 6.—Full-power peak beam current density as a function of time for “clean” staggered Faraday probes at axial positions of 20 and 173 mm.

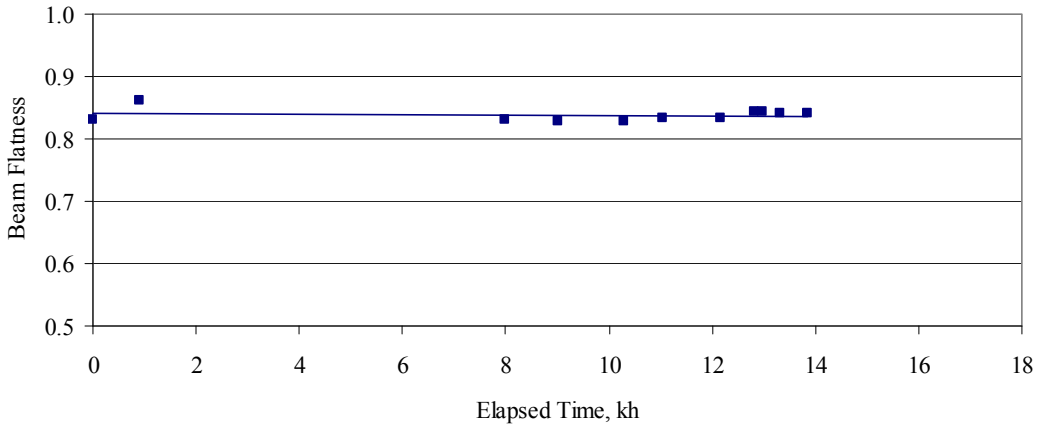

Figure 7.—Full-power beam flatness parameter as a function of time for “clean” Faraday probe at an axial position of 20 mm.

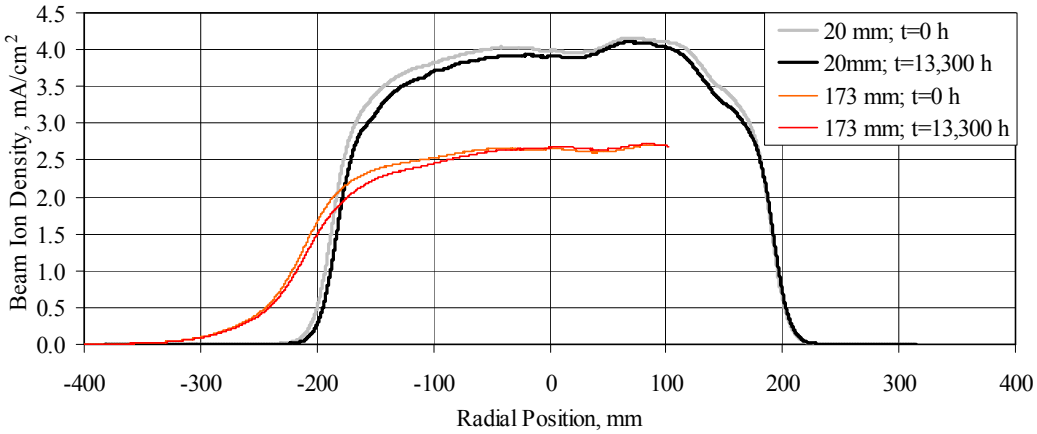

Figure 8.—Full-power thruster pretest and 13,300 h radial beam profiles at axial positions of 20 and 173 mm.

At full-power, the beam flatness parameter, defined as the ratio of average-to-peak ion current densities, has ranged from 0.82 to 0.86, over the duration of the test when analyzing only the "clean" probe sweeps. The average ion current density is calculated from the thruster beam current and the active beam extraction area at the thruster. The NEXT beam flatness is a considerable improvement over the NSTAR thruster that had a beam flatness of ~0.5 at full power (Refs. 25 and 48). Ion beam radial current density profiles at the various downstream locations from the ion optics are used to calculate beam divergence half-angles (Ref. 45). Beam divergence, defined as the half-angle containing 95 percent of the probe integrated current, has changed from 24.5° to 25.7° at full-power becoming slightly more divergent over the course of 13,800 h of operation, the last time all three Faraday probes were functional, due to enlargement of the accelerator apertures at large radii. The beam divergence calculation is also affected by the increasing collection area of the Faraday probe at the 238 mm downstream location.

Doubles-to-Singles Ratio

The ExB probe measures the doubles-to-singles signature in the far field over the duration of the test. The doubles-to-singles signatures as a function of elapsed time for sample operating conditions are plotted Figure 9 showing an increase at full-power from 0.08 to 0.10 over ~16,000 h. For reference the NSTAR ELT doubles-to-singles current ratio varied from 0.12 to 0.20 over the duration of the test (Refs. 26 and 28). The increase in the doubles-to-singles ratio at full-power for the LDT is caused by the increase in the discharge voltage observed during the wear test (Refs. 49 and 50). The change in doubles-to-singles by 0.02 for an ~ 1 V increase in discharge voltage is consistent with the sensitivity observed during the NSTAR ELT (Ref. 26). There has been no observed change in double-to-singles signature following throttling to the 4.7 kW operating condition.

Erosion Results

The discharge cathode assembly (DCA), neutralizer cathode assembly (NCA), accelerator grid center-radius aperture (CRA), mid-radius aperture (MRA)—located 16 cm radially from center, outer-radius apertures (ORA), and ion optics' cold grid-gap are imaged with their respective CCD cameras. The locations imaged by the CCD cameras are shown in Figure 10 along with the additional test hardware in the picture. The results of the erosion measurements are discussed in the following sections. Erosion images were taken every 200 h for the first 5,000 h and at least every 800 h afterwards.

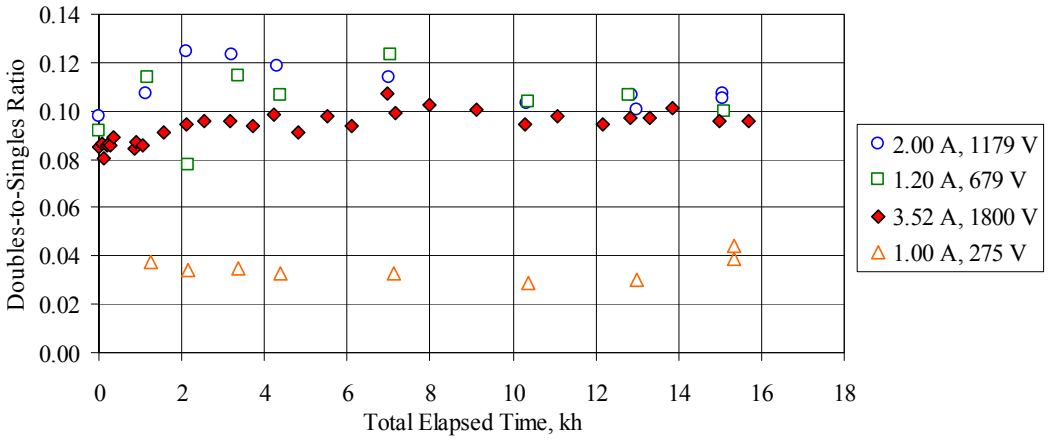

Figure 9.—Performance characterization doubles-to-singles signatures as a function of time.

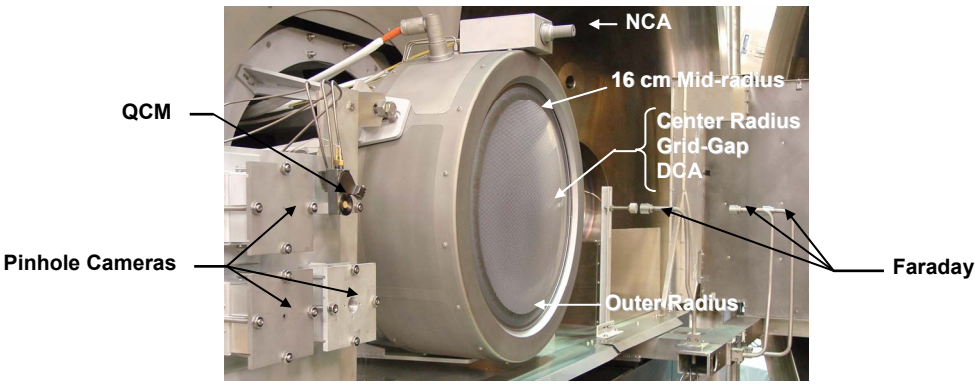

Figure 10.—Photograph of QCM, pinhole cameras, CCD image locations, and staggered Faraday probes.

Discharge Cathode Assembly (DCA)

Figure 11 shows the discharge cathode at 0, 11,700, and 16,550 h along with comparison photographs of the NSTAR ELT discharge cathode assembly. The NEXT discharge cathode faceplate has become slightly textured, but the discharge cathode orifice, cathode orifice chamfer, and keeper orifice diameters have not changed within the measurement error, as shown in Figure 12 normalized by the beginning-of-test values. There has not been a noticeable change in any of the discharge cathode assembly orifices as a result of the change in thruster operating condition to 4.7 kW or the shorting of the discharge keeper to cathode at high emission currents. During the NSTAR ELT, the keeper electrode was completely eroded away, exposing the discharge cathode and heater (Ref. 51). The NSTAR ELT keeper erosion was characterized by a widening of the keeper orifice in contrast to the NEXT 2,000 h and NSTAR 8,200 h wear tests, in which the most severe erosion was focused towards the mid-radius of the keeper faceplate (Refs. 17, 25, and 35). The primary function of the discharge cathode keeper is to protect the discharge cathode from excessive sputter erosion. The EM3 keeper material was changed to graphite, which has a sputter yield an order of magnitude lower than that of the molybdenum at 50 eV (Ref. 29). While the LDT results confirm that no enlargement of the keeper orifice has occurred, the erosion of the downstream face of the keeper is not measured in-situ. Discharge cathode keeper downstream surfaces from the NSTAR 8,200 h and NEXT 2,000 h wear tests were qualitatively similar with the deepest erosion at a radii of 55 to 60 and 40 percent of the total keeper radius, respectively(Refs. 17, 25, and 35). Scaling the NEXT 2,000 h wear test molybdenum discharge keeper erosion rate (depth of 17 percent of the keeper thickness after test) with the decrease in sputter yield of graphite compared to molybdenum gives a conservative estimate of wear through of the keeper after > 87 kh at full-power (>1800 kg) (Refs. 29, 35, and 52).

Shorting of the discharge keeper to common was observed in the NSTAR ELT and contributed to the anomalous erosion (Ref. 28). It was anticipated based upon the findings of the NEXT 2,000 h and HiPEP 2,000 h wear tests that a similar shorting event would occur during the NEXT LDT (Refs. 17 and 53). Post-test analyses measured material deposits on the upstream surface of the keeper faceplate near the orifice of 40 and 70 μm thicknesses for the NEXT and HiPEP wear tests, respectively (Refs. 53 and 54). Assuming linear growth, extrapolation of these thicknesses for extended duration would have resulted in bridging the estimated operating gap between the NEXT LDT keeper and cathode face after an operating duration on the order of 10 to 20 kh. The short appeared in the NEXT LDT after 13.9 kh, within the bounds of the two deposition rates. It should be mentioned that the NEXT lifetime assessment also predicted a priori this shorting event and considered its impact on thruster service life. (Refs. 20 and 42).

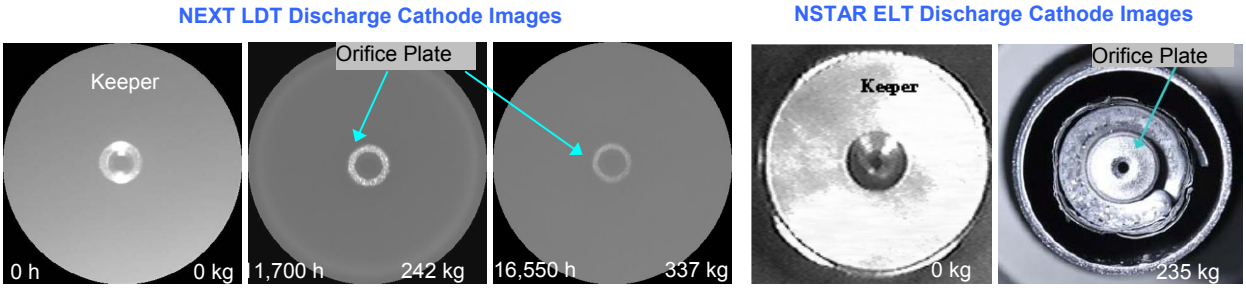

Figure 11.—Discharge cathode assembly images for NEXT LDT (left) and NSTAR ELT (right) (Refs. 26, 28, 51, and 56).

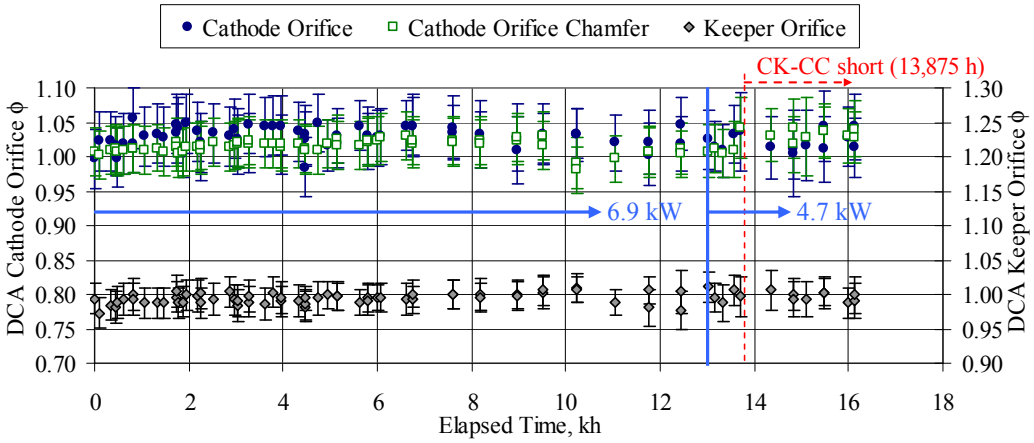

Figure 12.—NEXT discharge cathode orifice diameter, orifice chamfer diameter, and keeper orifice diameter normalized to pretest values as a function of time.

Neutralizer Cathode Assembly (NCA)

Figure 13 shows the NCA pretest and image taken after 16,550 h of thruster operation. Texturing of the neutralizer cathode faceplate is observed and a darkening of the keeper is seen due to back-sputtered carbon deposition from the facility. The NCA is located in the 12 o'clock position of the thruster so any erosion due to placement of the NCA in the high-energy beam would be seen in the bottom of the images taken, which appears pristine. Normalized measurements from the erosion images, shown in Figure 14, confirm no observed erosion of the NCA keeper orifice diameter or cathode orifice diameter, while the cathode orifice chamfer diameter has increased by ~20 percent over the test duration.

Though the neutralizer orifice does not show any erosion when imaging on centerline, it is likely that EM3 neutralizer orifice channel has a similar erosion profile to the NSTAR 8,200 h wear test and NSTAR ELT (Refs. 25 and 26). The image of the orifice is taken looking down the axis of the cathode and thus only will show the smallest diameter along the channel. The observed reduction in neutralizer flow margin with test duration suggests erosion of the orifice channel is occurring (Ref. 43). A slight increase in the chamfer dimension has been observed. A step increase of 10 percent in the chamfer dimension was observed after throttling to the 4.7 kW operating condition.

Accelerator Grid Apertures

Images of the CRA, 16 cm or mid-radius MRA, and ORA are obtained periodically throughout the wear test. Erosion of the CRA showed formation of a hexagonal groove pattern within the first few hundred hours of operation. Figure 15 illustrates the pre-test and latest CRA images. The hexagonal

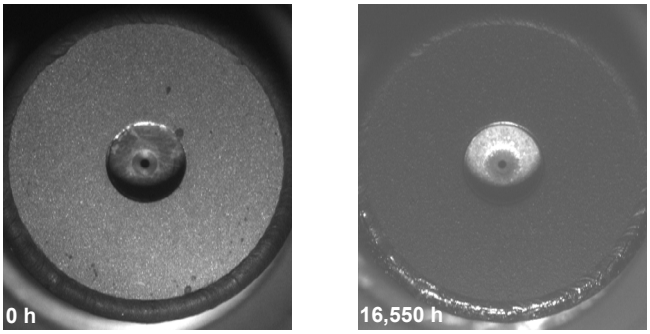

Figure 13.—Neutralizer assembly erosion images.

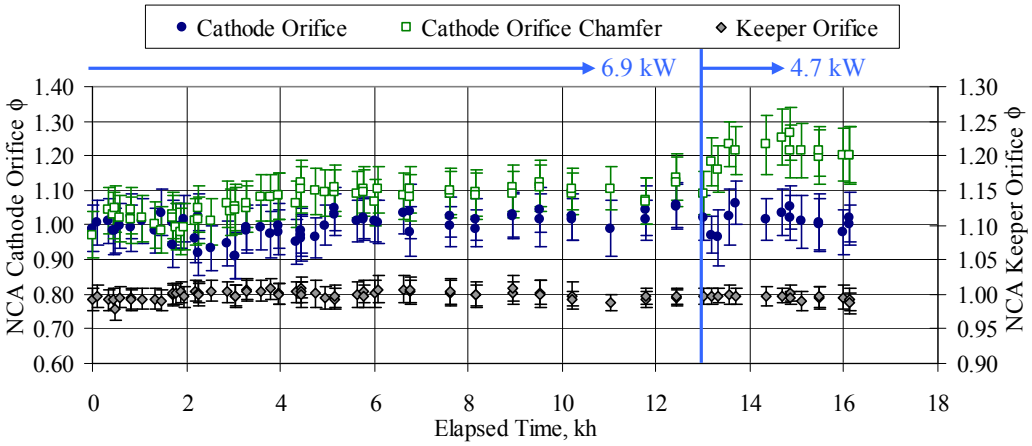

Figure 14.—Neutralizer cathode orifice diameter, orifice chamfer diameter, and keeper orifice diameter normalized to pretest values as a function of time.

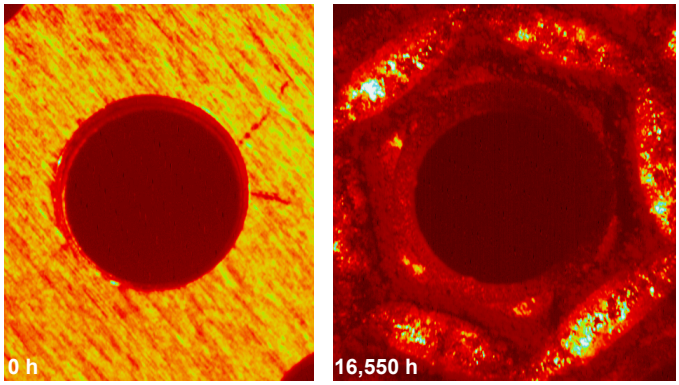

Figure 15.—Accelerator grid center-radius aperture images with an applied red palette.

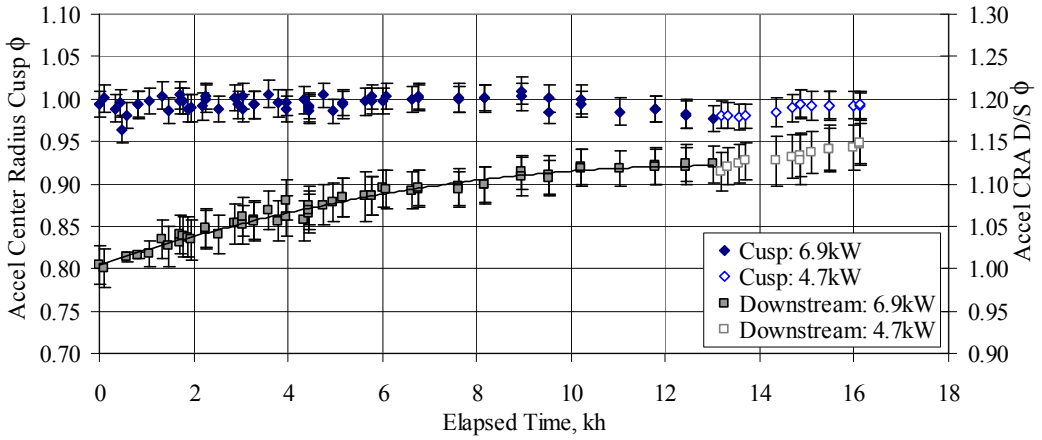

Figure 16.—Accelerator grid center-radius cusp diameter and downstream diameter normalized to pretest values as a function of time.

groove pattern is clearly evident as well as the buildup of back-sputtered carbon around the inside of the groove pattern. The CRA erosion measurements, normalized to the beginning-of-test value, are shown in Figure 16. Within the uncertainty of the measurement, no variation of CRA cusp has been detected. There was a 12 percent increase in the CRA downstream diameter after 13,042 h of full-power operation, which asymptoted to a final value for this operating condition. Since throttling to the 4.7 kW operating condition, the CRA cusp diameter has remained constant, but the downstream diameter has increased further. This increase in downstream diameter was predicted based upon the decrease in total voltage from full-power to 4.7 kW operating condition. The decrease in total voltage for approximately the same beamlet current density results in a less focused beamlet. Under-focusing of the beamlet results in an increase in the downstream erosion rate. This behavior and predictions of aperture erosion for alternate operating conditions is described in greater detail in Reference 20. It is anticipated that this downstream diameter will similarly asymptote to a final geometry. After 16,550 h, the CRA downstream diameter has increased by 15 percent.

The lack of CRA cusp enlargement in the NEXT LDT is in sharp contrast to the observed trend during the NSTAR ELT. Figure 17 shows the normalized CRA cusp measurements for the NEXT LDT and NSTAR ELT illustrating the difference in CRA cusp erosion (Ref. 26). The NEXT PM ion optics beginning-of-test erosion is characterized by aperture downstream chamfering compared to the NSTAR ion optics aperture cusp and downstream erosion. The difference is due to the more highly focused beamlets at the NEXT full-power and 4.7 kW operating conditions. Aperture cusp enlargement leads to increased neutral losses, more variable performance parameters, and possible electron back-streaming. CRA cusp diameter erosion is expected to be most severe at the 4.7 kW operating condition (i.e., highest beam current density with lowest total voltage) and since no CRA cusp erosion is observed it is anticipated that for all other operating conditions there will be negligible cusp erosion.

Images of the MRA illustrate net-deposition around this aperture located 16 cm from the grid centerline (i.e., 2 cm from outer apertures). The pre-test and most recent MRA images are shown in Figure 18. Groove erosion is trumped by the back-sputtered carbon deposition. The MRA cusp diameter increased only 2 to 3 percent after 13,042 h of full-power operation, equal to the measurement uncertainty. The downstream diameter has increased and the asymptoted to a final value after 9,000 h of operation as shown in Figure 19. After 13,042 h of operation at full-power the MRA downstream diameter increased by 10 percent. There has been no indication of cross-over impingement at the mid-radius location. Since throttling to the new operating condition, the MRA downstream diameter has increased further as anticipated, but is expected to asymptote to a final geometry. After 16,550 h, MRA cusp and downstream diameters are 4 and 15 percent larger than pretest, but appear to have asymptoted to their final values at the 4.7 kW operating condition.

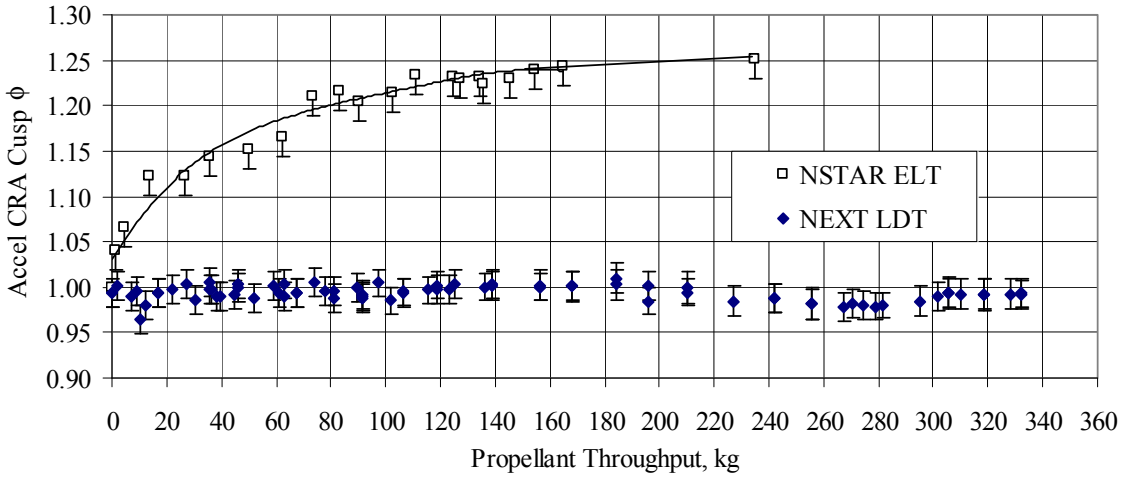

Figure 17.—Accelerator grid center-radius aperture cusp diameter for the NEXT LDT and NSTAR ELT (Refs. 26, 28, 51, and 56)

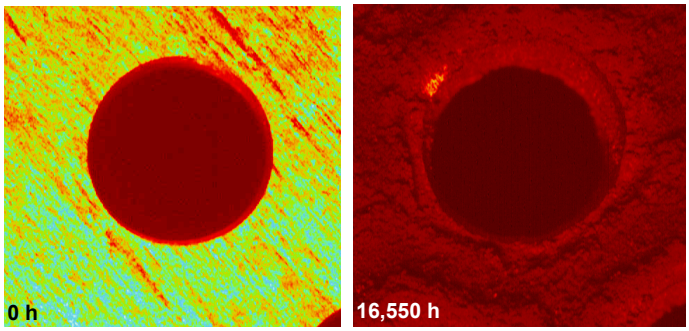

Figure 18.—Accelerator grid mid-radius aperture erosion images with an applied red palette.

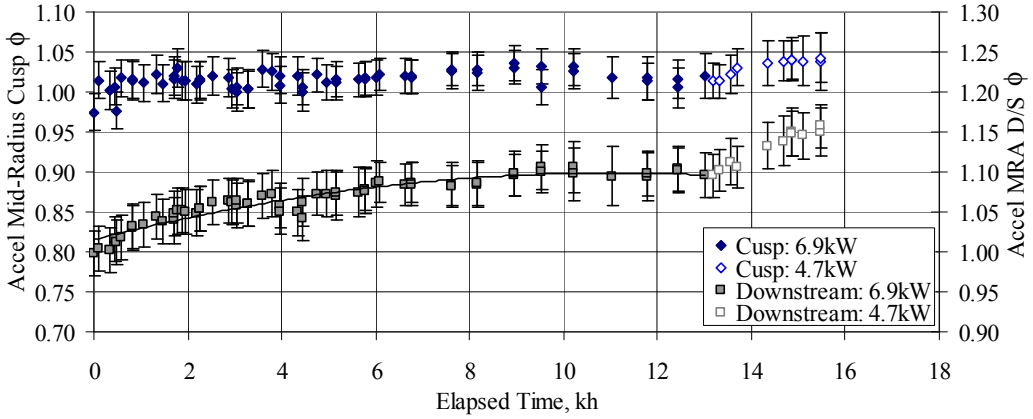

Figure 19.—Accelerator grid mid-radius cusp diameter and downstream diameter normalized to pretest values as a function of time.

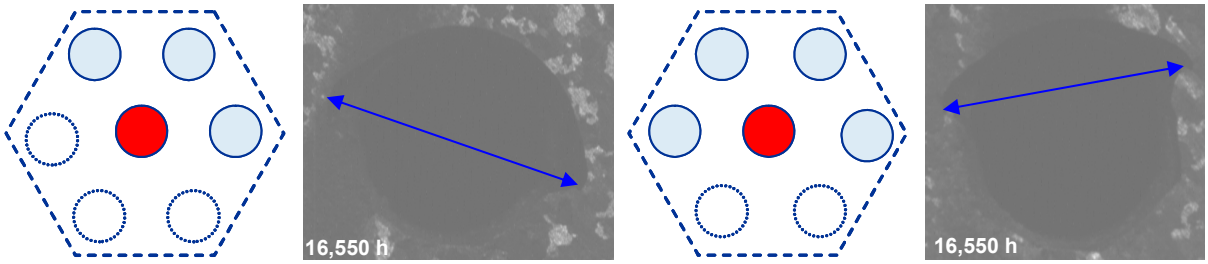

Figure 20.—Accelerator grid outer-radius aperture configurations and “ear” dimensions after 16,550 h. The imaged aperture is centered, shaded neighboring apertures are active and open apertures are closed.

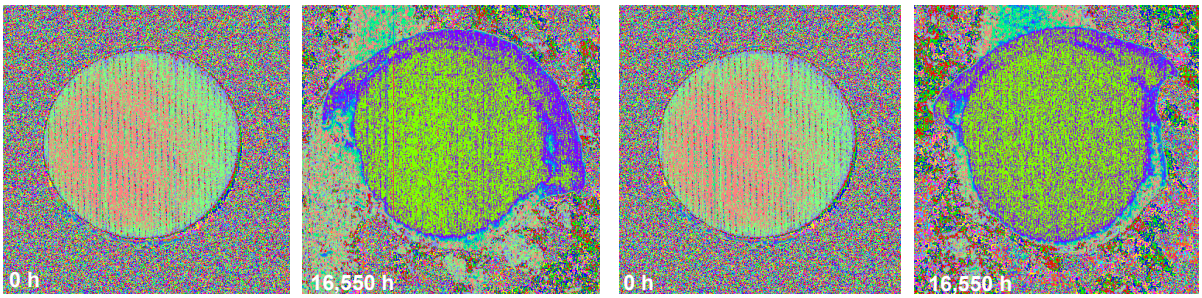

Figure 21.—Accelerator grid 3-neighbor outer-radius aperture images with applied palette (left) and 4-neighbor outer-radius aperture image with palette (right).

Images are taken of the four outer-radius apertures on the accelerator grid. The outer-radius apertures all have some neighboring apertures that are solid, i.e. not active. The presence of active and non-active apertures around outer-radius apertures results in different erosion patterns depending upon the configuration of the individual aperture. Three of the ORA’s imaged have identical configurations with 3-of-6 neighboring apertures active and the other 3 solid. The fourth ORA has 4-of-6 neighboring apertures active with 2 solid. The geometries of the ORA apertures and images of the ORA apertures after 16,550 h of operation are shown in Figure 20. The formation of “ear” erosion in the first few hundred hours of operation has been closely monitored to ensure that this erosion does not lead to significant structural degradation of accelerator grid. The “ear” formation results from over-focusing at the outer radius apertures due to the low discharge plasma densities at the large radii of the optics and the shape of the distorted sheath due to lack of neighboring apertures (Refs. 17, 21, and 22).

Erosion images of the ORA’s are shown in Figure 20 and Figure 21. Only one of the 3-neighbor outer-radius apertures is shown due to similarity. The 4-neighbor ORA exhibits a different “ear” erosion pattern. In both cases, the low-density and non-symmetric aperture sheath causes ions originating near missing aperture locations to crossover resulting in directly impingement (Refs. 22 and 55). Erosion measurements of the ORA’s are shown in Figure 22 illustrating minimal cusp erosion. Only one 3-neighbor aperture is shown in Figure 22 because the other two demonstrate equivalent erosion results. The “ear” dimensions, defined in the schematic in Figure 20, increased rapidly during the first 2,000 h of operation at full-power and the growth rate decreased substantially afterwards. The 3-neighbor ORA’s and 4-neighbor ORA “ear” dimensions have increased by ~40 and 25 percent, respectively. The “ear” erosion was expected based upon previous wear test results, most notably the NEXT 2,000 h WT, and from ion optics modeling (Refs. 17 and 22). The ORA erosion is shown to have a negligible impact on thruster performance and is not sufficient to cause structural degradation of the accelerator grid. Since throttling the thruster, there has been no observed change in the ORA geometries. It is not expected that the over-focusing erosion would increase until the thruster is operated at a condition that has a higher ratio of total voltage to beam current density, which on the NEXT throttling table is the highest value for the 1800 V beam power supply voltage and 1.20 A beam current (Ref. 20).

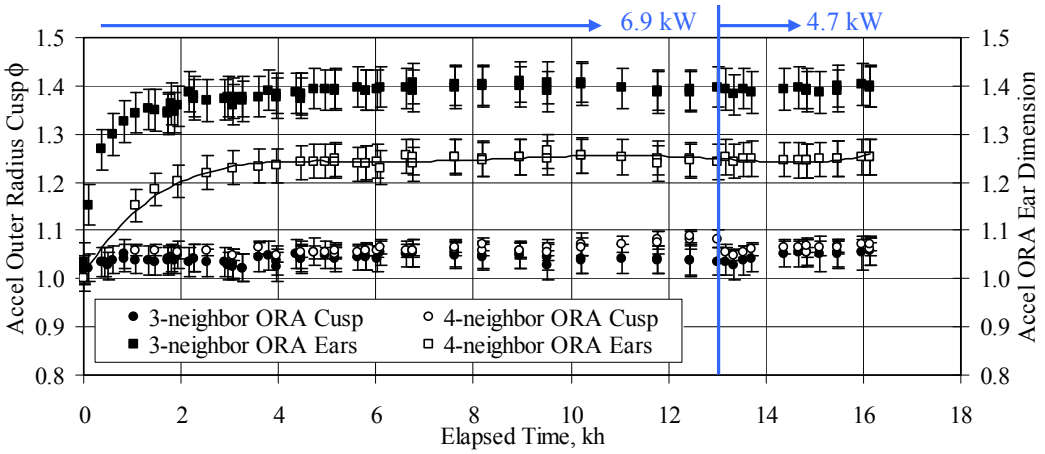

Figure 22.—Accelerator grid outer-radius cusp diameters and downstream "ear" dimensions normalized to pretest values.

Accelerator Groove Erosion

Erosion of the accelerator grid downstream surface by charge-exchange ions results in pit and groove formation and can lead to the eventual structural failure of the accelerator grid. During the NSTAR ELT, the accelerator pit depth was measured during the first 10,000 h of operation with laser profilometer. Problems with the diagnostic precluded accurate measurement of pit depth afterwards. The post-test inspection revealed pit erosion through the thickness of the accelerator grid (Ref. 26). NEXT 2,000 h WT post-test profilometer measurements indicated the deepest pit depth around the center radius aperture was 12 percent of the accelerator grid thickness. The center radius and deepest groove depths were 5 and 6 percent, respectively, with the maximum groove depth at the ¼-radius location (Ref. 21). To measure the NEXT LDT groove depth, a diagnostic technique was developed using the existing accelerator grid CCD cameras to determine the pit and groove depth at the center-radius location (Ref. 49).

There are no discernable pits at the center-radius location for the NEXT LDT as illustrated in the erosion images such as Figure 15 and Figure 23, however, grooves are clearly visible. The groove depth measurement has been obtained since 7,600 h of operation at least every 700 to 800 h and the results are presented in Figure 24. The measured increase in groove depth at full-power is consistent with the results from the NEXT 2,000 h WT and less than the NSTAR ELT pit depths for equivalent operating times, also shown in Figure 24 (Refs. 17, 21, 28, and 56). The groove erosion is expected to be linear with time, assuming operation at a fixed operating condition. Extrapolation of the groove depth trend at full-power, the most severe groove erosion as a function of hours of operation, indicate wear-through at a throughput of 700 to 800 kg. The wear-through of the accelerator grid does not in itself represent a failure of the thruster. Since throttling the thruster, a noticeable groove erosion rate decrease has been observed as expected. This change is consistent with the model incorporated by the NEXT thruster service life assessment also shown in Figure 24 (Refs. 20 and 42).

Application of a model developed to predict the effect of backsputtering on grid erosion, with a 3 μm/kh back-sputter rate and center-radius aperture ion impingement current density, estimates a maximum of 10 percent reduction in erosion near the beam center, where pit and groove erosion rate is highest, during the NEXT LDT due to back-sputtered carbon (Ref. 57). Additional analyses have been performed to predict the impact of the backsputtered carbon deposition on the accelerator grid utilizing the MICHELLE PIC-code (Ref. 58). The resulting analysis estimates a 30 percent reduction in the maximum groove erosion due to carbon deposition in the LDT (Ref. 58). From NSTAR data on DS1, the impingement accelerator current in space was ~25 percent less than the NSTAR data obtained during pre-flight measurements at 1.50 A beam current and 25.56 sccm total flow rate in a test facility operating with a background pressure level of 3.5×10^{-6} torr (Refs. 1, 26, and 59). The NEXT LDT is operating at

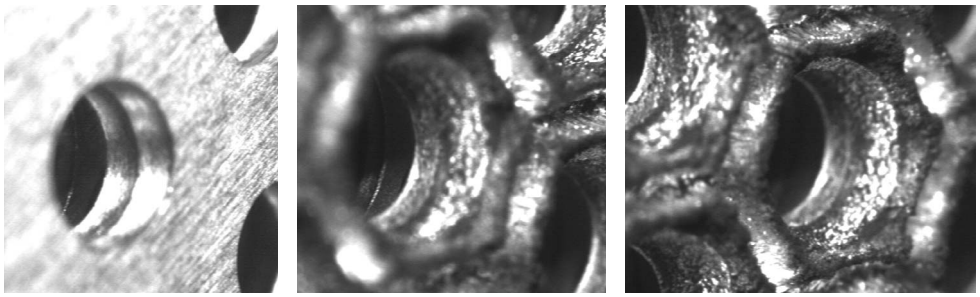

Figure 23.—Accelerator grid-gap aperture images: CRA at t = 0 (left), CRA at t = 16,550 h (middle), and ~1 in. off-center from CRA at t = 16,550 h (right).

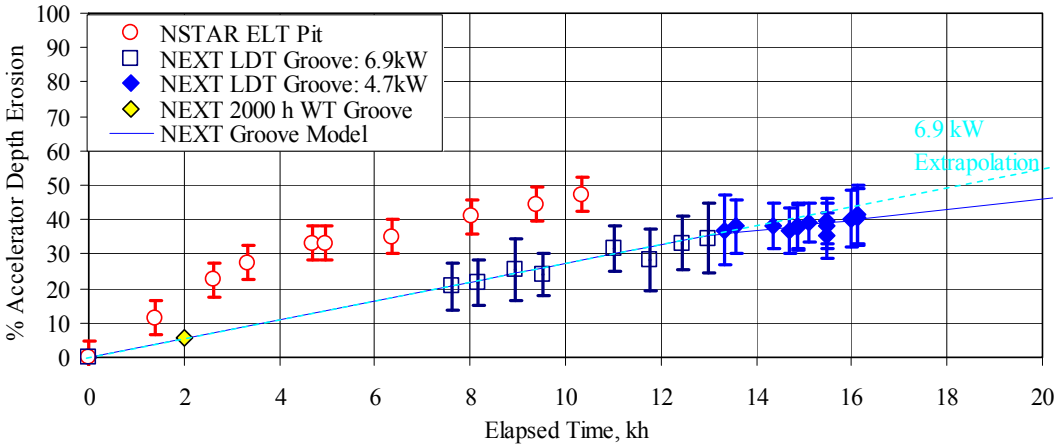

Figure 24.—NEXT LDT accelerator grid center-radius groove erosion depth, percentage of total accelerator grid thickness, as a function of time. Also shown is the post-test analysis of centerline groove depth from the NEXT 2,000 h WT and the NSTAR ELT pit depth with test duration (Refs. 17, 21, 26, and 56).

slightly higher operating background pressures at full-power, resulting in measured NEXT accelerator currents that would be ≥25 percent larger than those in space and therefore accelerator grid erosion would be approximately 25 percent less in space. The combined effects of elevated background pressure in the test facility and backsputtered carbon deposition essentially cancel out and therefore the LDT groove wear is expected to be representative of thruster operation in space.

Ion Optics Grid-Gap

The gap between the screen and accelerator grids decreased over the course of both the NSTAR ELT and 8,200 WT (Refs. 25 and 28). Pre- and post-test grid-gap measurements from the NSTAR ELT and 8,200 h wear test indicated 30 and 12 percent reduction in the cold grid-gap, respectively (Ref. 26). It is not known how the grid-gap varied over the course of the tests because no data is available. Analysis of electron backstreaming data indicates the grid-gap change probably occurred slowly over the duration of the test (Ref. 26). Decreases in grid-gap cause an increase the electric field between the grids resulting in reduced electron backstreaming margin and increased arcing between the grids. A decrease in the cold grid-gap of 7 percent was also observed following the NEXT 2,000 h wear test, which utilized EM ion optics. To address this undesirable change, the PM ion optics assembly and mounting scheme were modified from the EM design specifically to address and eliminate the observed decreasing cold grid-gap with thruster operation. A CCD camera images the centerline cold grid-gap periodically throughout the LDT. Within the measurement uncertainty, there has been no observed change in the NEXT LDT cold grid-gap, shown in Figure 25, which utilizes PM ion optics. This is supported by the lack of change in the electron backstreaming margin over the test duration.

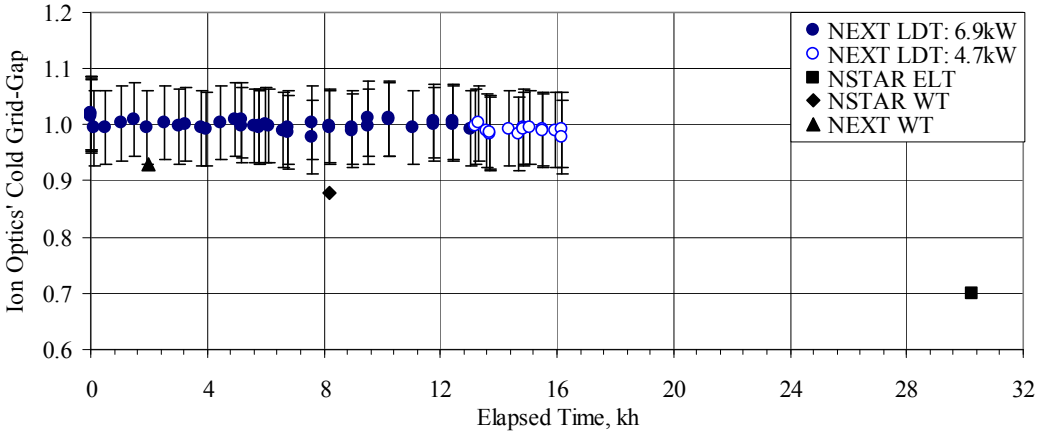

Figure 25.—Cold centerline grid-gap data for the NEXT LDT, NEXT 2kh WT, NSTAR ELT, and NSTAR 8,200 h WT normalized to beginning-of-test values (Refs. 17, 21, 25, 26, and 56).

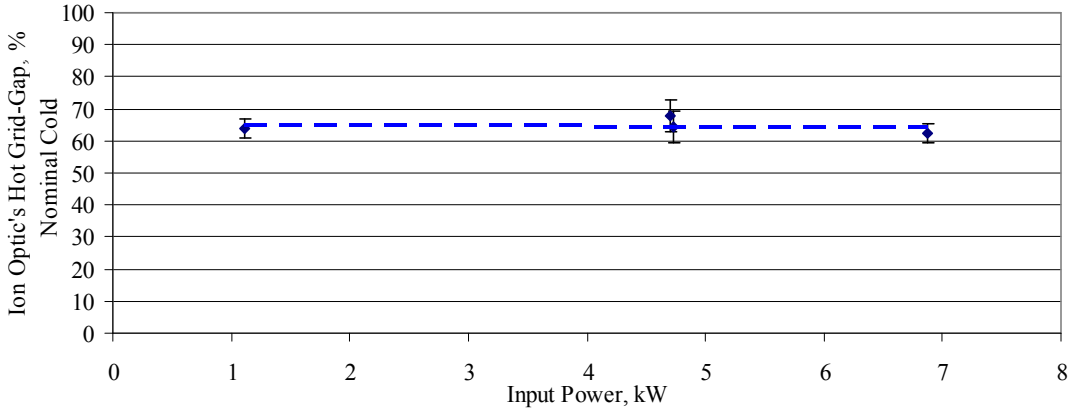

Figure 26.—enterline operating grid-gap data for the NEXT PM ion optics for various thruster operating conditions as indicated by thruster input power.

The thruster service life and ion optics modeling efforts require the hot ion optics' grid-gap as an input. The recent application of the MICHELLE PIC-code to the NEXT ion optics geometries has been combined with first-order regression and carbon deposition analyses allowing a secondary assessment of the effect of carbon deposition in the LDT. Uncertainty in the hot electrode spacing has resulted in large uncertainties in this modeling effort. To assist in this and future modeling efforts, an estimate of the centerline hot grid-gap of the NEXT EM3 thruster has been performed utilizing the in-situ grid-gap CCD used in the LDT. Measurements of the hot grid-gap on NSTAR thrusters had been previously made illustrating a hot grid-gap that was half of the cold grid-gap at full power (Ref. 60). There are a number of differences between the NEXT PM ion optics and NSTAR ion optics. The primary differences are: increased accelerator grid thickness, larger area of solid domed material outside of apertures, and improved grid mounting techniques to eliminate the buildup of stresses during assembly and better manage thermally induced stresses during operation. No hot grid-gap data had been obtained previously on the NEXT engine. Hot grid-gap images were obtained during the NEXT LDT immediately prior to and subsequent to the thruster shutdown for cooldown transient data. The operating data are shown for thruster operation at 3 different operating conditions in Figure 26. The operating hot grid-gap for NEXT PM ion optics appears to be insensitive to thruster input power as evident by the graph. A thermal development test conducted on the NEXT PM thruster revealed that the temperature delta between thermocouples located on the screen and accelerator grid mounts was also insensitive to thruster operating condition and therefore consistent with the hot grid gap measurement findings (Refs. 61 and 62). The data

reveal centerline hot grid-gap estimates to be 65 percent ± 3 percent of the cold centerline grid-gap, slightly larger than the 50 percent NSTAR gap at full power (Refs. 60 and 63). Transient comparison following thruster shutdown from full-power can be found in Reference 50.

Erosion Predictions and Thruster Life

Accelerator Grid Erosion

An integrated thruster performance and erosion model was developed to predict the erosion of critical NEXT components as a function of throttling profile. The model predicts the accelerator grid aperture erosion at the CRA, MRA, and ORA locations, accelerator groove depth penetration, and both discharge and neutralizer faceplate erosion and barium depletion. For this predicted erosion, thruster performance parameters such as discharge current, discharge losses, and electron backstreaming margin are predicted with thruster operating condition and predicted erosion as inputs. These predictions are made with thruster throttling profile, i.e., thruster operating conditions, duration, and sequence, as the input to the model. This modeling activity and the methodology behind it is described in detail in References 20 and 42. Some of the results for this modeling are shown in Figure 27. On the graph, the thruster operating conditions are referred to by an assigned throttle level, or TH level, for this paper only and not a universal designation. The operating parameters for the assigned throttle levels are defined in Table A.1.

Operation for extended duration at the full-input power, or TH 40, operating condition establishes the expected thruster service life capability as groove erosion, the lifetime limiter at all operating points, is most severe as a function of duration at full-power than any other operating condition on the NEXT throttle table. At the condition of high-beam current density and low total accelerating voltage, TH 19, CRA and MRA downstream and cusp erosion (if any) are most severe as the figure shows MRA downstream diameter further increasing past its final full-power geometry. It turns out that TH 19 is also the condition with the highest ratio of discharge cathode emission current to flow rate, which may have contributed to the NSTAR ELT anomalous keeper erosion. Operation at an intermediate power level, TH 8, is consistent with many of the potential NEXT mission profiles as well as throttling back up to full-power, consistent with inner solar system fly-by. For mission representation these operating conditions and their sequence are included. Operation at the lowest-power level, TH 1, is required to bound the NEXT throttle table and may illustrate potentially unmodeled phenomena such as neutralizer clogging. This operating condition is also the worst groove erosion as a function of throughput. Finally, operation at the condition of low-beam current density and high total voltage, TH 34, will have the most severe outer-radius aperture erosion due to over-focusing. These erosion predictions can be used to estimate depletion of electron backstreaming margin and the increase in required discharge current, and hence discharge losses, to maintain constant beam current as accelerator apertures enlarge. At the end of the planned NEXT LDT throttling profile the accelerator groove penetration is expected to reach 60 percent of the total accelerator grid thickness. Since this is the thruster life-limiter, there is 40 percent margin, or additional capability, after thruster operation for 27 kh and processing 460 kg of Xe. Note that groove penetration does not in itself represent a thruster failure.

Discharge Current and Discharge Losses Predictions

Increasing discharge currents during wear tests are required to maintain discharge chamber ion production, and hence beam current, as the neutral loss rate increases due to erosion of accelerator grid apertures (Refs. 26 and 64). A model was developed to predict the increase in discharge current required to maintain a given beam current based upon the observed and predicted trends in aperture erosion. Erosion of the majority of the accelerator apertures in the NEXT LDT, the exception being the ORA's, has been confined to changes in the downstream surface, with little if any increase in cusp diameters. The CRA, MRA, and ORA erosion measurements are used to estimate the increase in neutral transmission factor during the test to determine the required increase in discharge current to maintain the beam current. Details describing the model and equations used can be found in References 49 and 50.

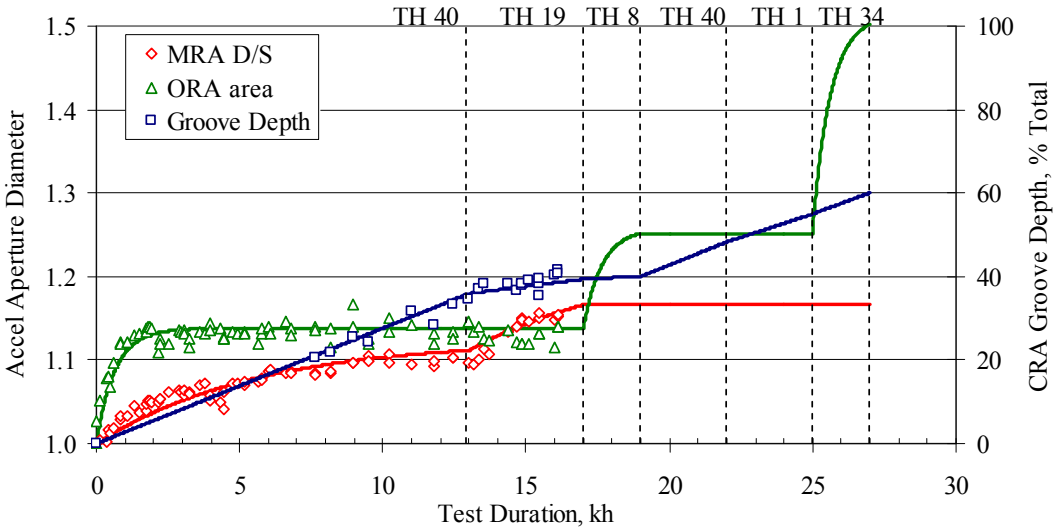

Figure 27.—EXT LDT accelerator aperture erosion predictions, normalized to beginning-of-life (BOL) values, and groove erosion depth for various thruster operating conditions as indicated by thruster (TH Level).

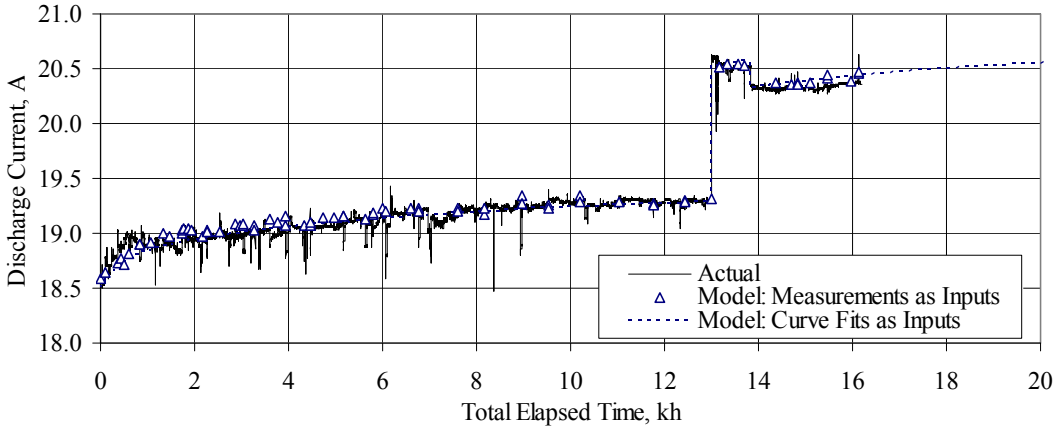

Figure 28.—Calculated discharge current from actual accelerator aperture images, predicted discharge current from aperture erosion curve-fit equations, and actual discharge current runtime data to date.

The discharge current calculated utilizing the above model with the measured aperture geometries as inputs is plotted as a function of time with the actual discharge current runtime data in Figure 28. The model accurately predicts the discharge current based upon the eroded geometries. During the first few hundred hours, the increasing discharge current is dominated by the ear formation in the outer-radius apertures seen as a sharp increase. Also shown in Figure 28 is a predicted trend for discharge current based upon curve fitting to the observed erosion of the apertures and extrapolation of the accelerator aperture erosion trends. The predicted discharge current after 450 kg processed at full-power is expected to increase by ~1.2 A using this technique. Discharge current during the NSTAR ELT increased by ~1 A, an equivalent of ~7 percent, over the test duration (Ref. 26).

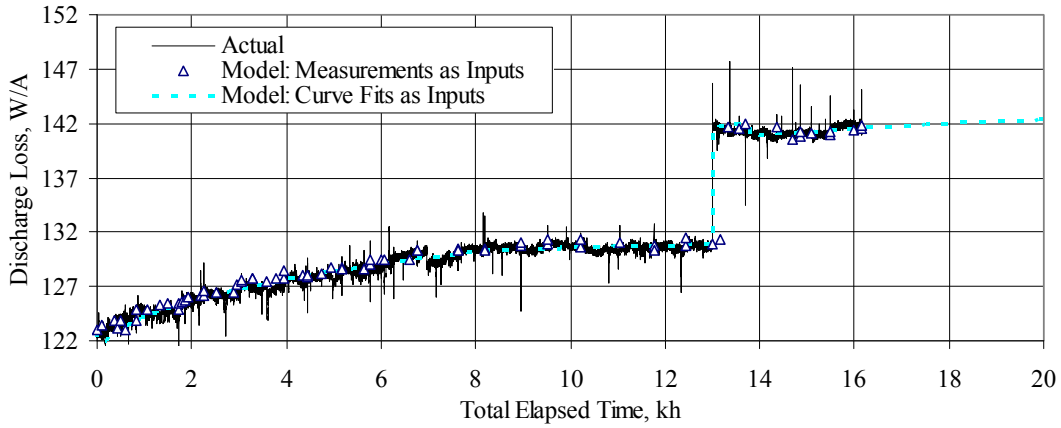

Figure 29.—Calculated discharge losses from actual accelerator aperture images and discharge voltage data, predicted discharge losses from aperture and discharge voltage curve-fit equations and extrapolations, and measured discharge loss runtime data as a function of time to date.

Discharge losses can also be estimated based upon the discharge current model results and the observed discharge voltage trends. Discharge losses are calculated according to Eq. (1) with discharge current calculated based upon accelerator erosion geometries. Discharge current and voltage step-changes due to shorting of the keeper to cathode are taken from observed data. The calculated discharge losses based upon this method agree well with the actual measured discharge losses, as can be seen in Figure 29. Extrapolating the observed discharge voltage trend and incorporating the predicted discharge current model, it is possible to predict future discharge losses.

$$\text{Discharge Loss} = \text{Discharge Loss}_{t=0} \times \left(\frac{V_{DC}}{V_{DC}\big|_{t=0}} \right) \left(\frac{J_{DC}}{J_{DC}\big|_{t=0}} \right) \tag{1}$$

Throttling of the thruster to alternate power levels will alter erosion patterns and rates. Predictions for aperture erosion rates are scaled for alternate operating conditions based upon the ratio of local perveance fraction at the new operating condition compared to the full-power operating condition. Substituting curve fits and extrapolation for the CRA, MRA, ORA, and discharge voltages, into the discharge current and discharge losses predicting equations, the predicted discharge loss curve, shown in Figure 29, is produced. The estimate for discharge losses, if the thruster was solely operated at full-power would reach 134 W/A after 450 kg of Xe processed, an increase of 11 W/A or ~9 percent of the beginning of test value. The behavior of the discharge voltage over long test durations is somewhat uncertain, based upon NSTAR wear test results (Ref. 26). During the NSTAR ELT, discharge voltage actually decreased by ~1 V at the same time as the keeper-to-common short appeared (Ref. 28). Thus, the NSTAR ELT discharge voltage data is not useful in predicting NEXT trends. If the NEXT LDT was conducted solely at full-power, the discharge losses would increase by 11 W/A after 450 kg compared to the NSTAR ELT full-power discharge losses increase of 22 W/A after 210 kg propellant processed.

Discharge Keeper Erosion

As mentioned previously, the onset of a short between the discharge cathode keeper and cathode common was expected based on previous NSTAR wear tests and is anticipated for the Dawn spacecraft NSTAR thrusters, which have not mitigated this issue. The onset of the short matches particularly well the extrapolation of deposition of material from the HiPEP 2 kh WT that used a graphite keeper (Ref. 53). Post-test analysis of the discharge cathode keeper during this wear test can also be used to conservatively

estimate the NEXT keeper life in a shorted configuration. Following completion of the HiPEP wear test, post-test inspection of the graphite keeper revealed negligible erosion with machining marks still visible. Measurements with a laser profilometer could not detect any keeper faceplate erosion within its resolution of 1 μm and accuracy of 10 μm. The operating condition for the HiPEP 2 kh WT had a discharge voltage of 28 V ± 1 V and discharge keeper to common voltage of ~4 V giving ~24 V ion energies impinging on the discharge keeper faceplate. Since similar electronics were used in both of the power consoles, it is anticipated that similar discharge voltage oscillations are present in the two thrusters. Given the uncertainty in the profilometer measurements, the maximum discharge keeper faceplate erosion rate from the HiPEP wear test is 5 μm/kh. Since the NEXT LDT discharge voltage is ~ 24.5 V at the 4.7 kW operating condition, with the keeper shorted to cathode common, a very close ion energy is expected for the NEXT LDT compared to the HiPEP 2 kh WT. Extrapolation with a erosion rate of 5 μm/kh to wear-through of the discharge keeper at 3.52 A, 1179 V gives hundreds of thousands of hours and thousands of kg throughput capability, i.e., much more than adequate life from the graphite keeper.

Conclusion

The results of the NEXT Long-Duration Test (LDT) as of June 25, 2008, are presented. The NEXT EM3 thruster has accumulated 16,550 h of operation, processed 337 kg of Xe, and demonstrated a total impulse of 13.3×10^6 N·s. *The NEXT thruster has surpassed the total throughput demonstrated by any ion thruster including the NSTAR flight spare thruster used in the extended life test. The NEXT LDT total impulse is the highest ever demonstrated by an ion thruster.* Thruster performance is characterized periodically over the throttling range of 0.5 to 6.9 kW, with calculated thrust of 26 to 237 mN, respectively. Overall thruster performance, which includes thrust, input power, specific impulse, and thrust efficiency, has remained constant with no signs of degradation.

Beam current density profiles have not changed significantly during the wear test. Beam divergence calculations, the half-angle containing 95 percent of the beam current, increased from 24.5° to 25.7° over the duration of the test due to accelerator aperture erosion at large radii and increased Faraday probe collection area for the furthest downstream location. The doubles-to-singles signature has decreased by a few percentage points over the entire test duration for most operating conditions, consistent with the increase in discharge voltage and the observed sensitivity of doubles-to-singles ratio to discharge voltage from other wear tests.

Images of the discharge and neutralizer cathode assemblies indicate, within the accuracy of the measurement, that the discharge and neutralizer cathode keeper and cathode orifice diameters have not changed. Erosion of center-radius and mid-radius accelerator apertures is primarily restricted to chamfering of the downstream diameter with increases in the cusp diameters that are slightly larger than the measurement uncertainty. The center-radius and mid-radius downstream diameters asymptoted to final values after ~9,000 h of full-power operation. Erosion of the outer-radius apertures demonstrate "ear" formation due to over-focusing at these low plasma density regions resulting in impingement on the accelerator grid with a greatly reduced erosion rate after ~ 2,000 h of operation. The "ear" formation at edge apertures was expected, has had a negligible impact thruster performance, and does not represent a structural concern to the accelerator grid. Since throttling to the 4.7 kW operating condition, there has been negligible cusp erosion observed, an increase in center and mid-radius downstream diameters that appears to by asymptoting to final values at this operating condition, and no observed change in outer-radius aperture geometries. Since the 4.7 kW operating condition is predicted to have the most severe under-focusing at the center and mid-radius locations, very little change of the center and mid-radius aperture geometries is expected for the remaining test segments.

There has been no change in the ion optics' cold grid-gap at centerline over the duration of the test validating the design changes made in the NEXT PM ion optics assembly to manage thermal stresses. The hot centerline grid-gap at full power is estimated to be 65 percent ± 3 percent of the cold grid-gap and insensitive to thruster operating condition. Groove formation was evident during the first few hundred hours of operation at the center radius location. The estimate for the groove depth at the center radius

aperture is ~40 percent of the accelerator grid thickness after 337 kg of Xe throughput. Extrapolation of groove depth at the center radius at full-power to complete wear through is consistent with the NEXT service life model value of 700 to 800 kg.

All thruster performance and erosion trends indicate that the NEXT thruster will achieve the qualification propellant throughput of 450 kg. Many of the high-risk NSTAR wear test erosion mechanisms and potential failure modes have been reduced or mitigated in the NEXT thruster, confirmed by in-situ measurements. An integrated thruster performance and erosion model has been developed using the NEXT LDT data and thruster service life assessment model to predict erosion of critical components and corresponding performance changes as a function of thruster throttling profile. The model shows good agreement with the NEXT LDT data.

Appendix

TABLE A.1.—NEXT ION THRUSTER THROTTLE TABLE WITH LDT PERFORMANCE OPERATING CONDITIONS SUBSET SHADED
[Full-power wear test condition in bold.]

TH level	P_{IN}, kW[a]	J_B, A	V_B, V	V_A, V	m_M, sccm	m_C, sccm	m_N, sccm	J_{NK}, A
40	**6.83**	**3.52**	**1800**	**–210**	**49.6**	**4.87**	**4.01**	**3.00**
33	6.03	3.52	1570	–210	49.6	4.87	4.01	3.00
26	5.43	3.52	1400	–210	49.6	4.87	4.01	3.00
19	4.68	3.52	1180	–200	49.6	4.87	4.01	3.00
39	6.03	3.10	1800	–210	43.5	4.54	4.01	3.00
32	5.32	3.10	1570	–210	43.5	4.54	4.01	3.00
25	4.80	3.10	1400	–210	43.5	4.54	4.01	3.00
18	4.14	3.10	1180	–200	43.5	4.54	4.01	3.00
38	5.27	2.70	1800	–210	37.6	4.26	3.50	3.00
31	4.65	2.70	1570	–210	37.6	4.26	3.50	3.00
24	4.19	2.70	1400	–210	37.6	4.26	3.50	3.00
17	3.61	2.70	1180	–200	37.6	4.26	3.50	3.00
12	3.20	2.70	1020	–175	37.6	4.26	3.50	3.00
37	4.60	2.35	1800	–210	32.4	4.05	3.50	3.00
30	4.06	2.35	1570	–210	32.4	4.05	3.50	3.00
23	3.66	2.35	1400	–210	32.4	4.05	3.50	3.00
16	3.16	2.35	1180	–200	32.4	4.05	3.50	3.00
11	2.80	2.35	1020	–175	32.4	4.05	3.50	3.00
36	4.00	2.00	1800	–210	25.8	3.87	2.50	3.00
29	3.54	2.00	1570	–210	25.8	3.87	2.50	3.00
22	3.20	2.00	1400	–210	25.8	3.87	2.50	3.00
15	2.77	2.00	1180	–200	25.8	3.87	2.50	3.00
10	2.46	2.00	1020	–175	25.8	3.87	2.50	3.00
35	3.24	1.60	1800	–210	20.0	3.70	2.75	3.00
28	2.87	1.60	1570	–210	20.0	3.70	2.75	3.00
21	2.60	1.60	1400	–210	20.0	3.70	2.75	3.00
14	2.26	1.60	1180	–200	20.0	3.70	2.75	3.00
9	2.01	1.60	1020	–175	20.0	3.70	2.75	3.00
34	2.43	1.20	1800	–210	14.2	3.57	3.00	3.00
27	2.15	1.20	1570	–210	14.2	3.57	3.00	3.00
20	1.95	1.20	1400	–210	14.2	3.57	3.00	3.00
13	1.70	1.20	1180	–200	14.2	3.57	3.00	3.00
8	1.51	1.20	1020	–175	14.2	3.57	3.00	3.00
7	1.41	1.20	936	–150	14.2	3.57	3.00	3.00
6	1.31	1.20	850	–125	14.2	3.57	3.00	3.00
5	1.11	1.20	679	–115	14.2	3.57	3.00	3.00
4	1.08	1.20	650	–144	14.2	3.57	3.00	3.00
3	0.777	1.20	400	–394	14.2	3.57	3.00	3.00
2	0.656	1.20	300	–525	14.2	3.57	3.00	3.00
1	0.529	1.00	275	–500	12.3	3.52	3.00	3.00

[a]Nominal values.

References

1. Polk, J.E., et al., "Performance of the NSTAR Ion Propulsion System on the Deep Space One Mission," AIAA–2001–0965, 39th AIAA Aerospace Sciences Meeting and Exhibit Joint Propulsion Conference, Reno, NV, Jan. 8–11, 2001.
2. Rayman, M.D., "The Successful Conclusion of the Deep Space 1 Mission: Important Results Without a Flashy Title," Space Technology, vol. 23, pp. 185–196, 2003.
3. Lee, M., et al., "Deep Space 1 Mission and Observation of Comet Borrelly," Deep Space 1 Mission and Observation of Comet Borrelly, 45th IEEE International Midwest Symposium on Circuits and Systems, Tulsa, OK, Aug. 4, 2002.
4. Brophy, J.R., et al., "Ion Propulsion System (NSTAR) DS1 Technology Validation Report," JPL Publication 00–10, Oct. 1999.
5. Oh, D., et al., "Deep Space Mission Applications for NEXT: NASA's Evolutionary Xenon Thruster," AIAA–2004–3806, 40th AIAA/ASME/SAE/ASEE Joint Propulsion Conference and Exhibit, Fort Lauderdale, FL, Jul. 11–14, 2004.
6. Oleson, S., et al., "Mission Advantages of NEXT: NASA's Evolutionary Xenon Thruster," AIAA–2002–3969, 38th AIAA/ASME/SAE/ASEE Joint Propulsion Conference and Exhibit, Indianapolis, IN, Jul. 7–10, 2002.
7. Patterson, M.J. and Benson, S.W., "NEXT Ion Propulsion System Development Status and Performance," AIAA–2007–5199, 43rd AIAA/ASME/SAE/ASEE Joint Propulsion Conference and Exhibit, Cincinnati, OH, Jul. 8–11, 2007.
8. Patterson, M.J. and Benson, S.W., "NEXT Ion Propulsion System Development Status and Capabilities," Conference Proceedings and NASA/TM—2008-214988, 2007 NASA Science Technology Conference, College Park, MD, Jun. 19–21, 2007.
9. Patterson, M.J., et al., "NEXT: NASA'S Evolutionary Xenon Thruster Development Status," AIAA–2003–4862, 39th AIAA/ASME/SAE/ASEE Joint Propulsion Conference and Exhibit, Huntsville, AL, Jul. 20–23, 2003.
10. Snyder, J.S., et al., "Single-String Integration Test Measurements of the NEXT Ion Engine Plume," AIAA–2004–3790 and NASA/TM—2005-213196, 40th AIAA/ASME/SAE/ASEE Joint Propulsion Conference and Exhibit, Fort Lauderdale, FL, Jul. 11–14, 2004.
11. Patterson, M.J., et al., "NEXT Ion Propulsion System: Single-String Integration Test Results," JANNAF Proceedings, Las Vegas, NV, May 2004.
12. Benson, S.W., et al., "NASA's Evolutionary Xenon Thruster (NEXT) Phase 2 Development Status," AIAA–2005–4070, 41st AIAA/ASME/SAE/ASEE Joint Propulsion Conference and Exhibit, Tucson, AZ, Jul. 10–13, 2005.
13. Pinero, L.R., et al., "Integration and Qualification of the NEXT Power Processing Unit," AIAA–2007–5214, 43rd AIAA/ASME/SAE/ASEE Joint Propulsion Conference and Exhibit, Cincinnati, OH, Jul. 8–11, 2007.
14. Monheiser, J., et al., "Development of a Ground Based Digital Control Interface Unit (DCIU) for the NEXT Propulsion System," AIAA–2004–4112, 40th AIAA/ASME/SAE/ASEE Joint Propulsion Conference and Exhibit, Fort Lauderdale, FL, Jul. 11–14, 2004.
15. Aadland, R.S., et al., "Development Status of the NEXT Propellant Management System," AIAA–2004–3974, 40th AIAA/ASME/SAE/ASEE Joint Propulsion Conference and Exhibit, Fort Lauderdale, FL, Jul. 11–14, 2004.
16. Snyder, J. S., et al., "Vibration Test of a Breadboard Gimbal for the NEXT Ion Engine," AIAA–2006–4665, 42nd AIAA/ASME/SAE/ASEE Joint Propulsion Conference and Exhibit, Sacramento, CA, July 9–12, 2006.
17. Soulas, G. C., et al., "NEXT Ion Engine 2000 Hour Wear Test Results," AIAA–2004–3791, 40th AIAA/ASME/SAE/ASEE Joint Propulsion Conference and Exhibit, Fort Lauderdale, FL, July 11–14, 2004.

18. Van Noord, J.L. and Williams, G.J., "Lifetime Assessment of the NEXT Ion Thruster," AIAA–2007–5274, 43rd AIAA/ASME/SAE/ASEE Joint Propulsion Conference and Exhibit, Cincinnati, OH, Jul. 8–11, 2007.
19. Herman, D.A., et al., "NASA's Evolutionary Xenon Thruster (NEXT) Component Verification Testing," AIAA–2008–4812, 44th AIAA/ASME/SAE/ASEE Joint Propulsion Conference and Exhibit, Hartford, CT, Jul. 21–23, 2008.
20. Van Noord, J.L. and Herman, D.A., "Application of the NEXT Ion Thruster Lifetime Assessment to Thruster Throttling," AIAA–2008–4526, 44th AIAA/ASME/SAE/ASEE Joint Propulsion Conference and Exhibit, Hartford, CT, Jul. 21–23, 2008.
21. Kamhawi, H., et al., "NEXT Ion Engine 2000 hour Wear Test Plume and Erosion Results," AIAA–2004–3792, 40th AIAA/ASME/SAE/ASEE Joint Propulsion Conference and Exhibit, Fort Lauderdale, FL, Jul. 11–14, 2004.
22. Malone, S.P., "Investigation of NEXT Ion Optics Erosion Processes using Computational Modeling," 2005–0356DV, NASA Glenn Research Center, Cleveland, OH, Oct. 20, 2005.
23. Herman, D.A., et al., "Performance Evaluation of the Prototype-Model NEXT Ion Thruster," AIAA–2007–5212, 43rd AIAA/ASME/SAE/ASEE Joint Propulsion Conference and Exhibit, Cincinnati, OH, Jul. 8–11, 2007.
24. Hoskins, W.A., et al., "Development of a Prototype Model Ion Thruster for the NEXT System," AIAA–2004–4111, 40th AIAA/ASME/SAE/ASEE Joint Propulsion Conference and Exhibit, Fort Lauderdale, FL, Jul. 11–14, 2004.
25. Polk, J.E., et al., "An Overview of the Results from an 8200 Hour Wear Test of the NSTAR Ion Thruster," AIAA–1999–2446, 35th AIAA/ASME/SAE/ASEE Joint Propulsion Conference and Exhibit, Los Angeles, CA, Jun. 20–24, 1999.
26. Sengupta, A., et al., "The 30,000-Hour Extended-Life Test of the Deep Space 1 Flight Spare Ion Thruster," NASA/TP—2004-213391, The Jet Propulsion Laboratory and NASA Glenn Research Center, Pasadena, CA, Mar. 2005.
27. Polk, J.E., et al., "A 1000 Hour Wear Test of the NASA NSTAR Ion Thruster," AIAA–1996–2784, 32nd AIAA/ASME/SAE/ASEE Joint Propulsion Conference and Exhibit, Lake Buena Vista, FL, Jul. 1–3, 1996.
28. Sengupta, A., et al., "An Overview of the Results from the 30,000 Hr Life Test of Deep Space 1 Flight Spare Engine," AIAA–2004–3608, 40th AIAA/ASME/SAE/ASEE Joint Propulsion Conference and Exhibit, Fort Lauderdale, FL, July 11–14, 2004.
29. Doerner, R.P., et al., "Sputtering Yield Measurements during Low Energy Xenon Plasma Bombardment," Journal of Applied Physics, Vol. 93, No. 9, pp. 5816–5823, May 1, 2003.
30. Sovey, J., et al., "Retention of Sputtered Molybdenum on Ion Engine Discharge Chamber Surfaces," IEPC Paper 2001–086, 27th International Electric Propulsion Conference, Pasadena, CA, Oct. 15–19, 2001.
31. Soulas, G.C. and Patterson, M.J., "NEXT Ion Thruster Performance Dispersion Analyses," AIAA–2007–5213, 43rd AIAA/ASME/SAE/ASEE Joint Propulsion Conference and Exhibit, Cincinnati, OH, July 8–11, 2007.
32. Soulas, G.C., et al., "Performance Evaluation of the NEXT Ion Engine," AIAA–2003–5278, 39th AIAA/ASME/SAE/ASEE Joint Propulsion Conference and Exhibit, Huntsville, AL, July 20–23, 2003.
33. Patterson, M.J., et al., "NEXT: NASA's Evolutionary Xenon Thruster," AIAA–2002–3832, 38th AIAA/ASME/SAE/ASEE Joint Propulsion Conference and Exhibit, Indianapolis, IN, July 7–10, 2002.
34. Frandina, M.M., et al., "Status of the NEXT Ion Thruster Long Duration Test," AIAA–2005–4065, 41st AIAA/ASME/SAE/ASEE Joint Propulsion Conference and Exhibit, Tucson, AZ, July 10–13, 2005.

35. Kamhawi, H., et al., “NEXT Ion Engine 2000 hour Wear Test Plume and Erosion Results,” AIAA–2004–3792, 40th AIAA/ASME/SAE/ASEE Joint Propulsion Conference and Exhibit, Fort Lauderdale, FL, Jul. 11–14, 2004.
36. Hickman, T.A., et al., “Overview of the Diagnostics for the NEXT Long Duration Test,” AIAA–2005–4064, 41st AIAA/ASME/SAE/ASEE Joint Propulsion Conference and Exhibit, Tucson, AZ, Jul. 10–13, 2005.
37. Pinero, L.R., et al., “Power Console Development for NASA's Electric Propulsion Outreach Program,” IEPC Paper 93–250, 23rd International Electric Propulsion Conference, Seattle, WA, Sep. 13–16, 1993.
38. Brophy, J.R., et al., “The Ion Propulsion System for Dawn,” AIAA–2003–4542, 39th AIAA/ASME/SAE/ASEE Joint Propulsion Conference and Exhibit, Huntsville, AL, Jul. 20–23, 2003.
39. Brophy, J.R., et al., “Status of the Dawn Ion Propulsion System,” AIAA–2004–3433, 40th AIAA/ASME/SAE/ASEE Joint Propulsion Conference and Exhibit, Fort Lauderdale, FL, Jul. 11–14, 2004.
40. Myers, R.M., “Proceedings of the Nuclear Electric Propulsion Workshop, Volume 1: Introductory Material and Thruster Concepts, Section: MPD Thruster Technology,” JPL D–9512 vol. 1, Jun. 19–22, 1990.
41. Herman, D.A., et al., “NEXT Long-Duration Test Plume and Wear Characteristics after 16,550 h of Operation and 337 kg of Xenon Processed,” AIAA–2008–4919, 44th AIAA/ASME/SAE/ASEE Joint Propulsion Conference and Exhibit, Hartford, CT, Jul. 21–23, 2008.
42. Van Noord, J.L., “Lifetime Assessment of the NEXT Ion Thruster,” AIAA–2007–5274, 43rd AIAA/ASME/SAE/ASEE Joint Propulsion Conference and Exhibit, Cincinnati, OH, Jul. 8–11, 2007.
43. Herman, D.A., et al., “Performance Characteristics of the NEXT Long-Duration Test after 16,550 h and 337 kg of Xenon Processed,” AIAA–2008–4527, 44th AIAA/ASME/SAE/ASEE Joint Propulsion Conference and Exhibit, Hartford, CT, Jul. 21–23, 2008.
44. Soulas, G.C., “Performance Evaluation of Titanium Ion Optics for the NSA 30 cm Ion Thruster,” IEPC–01–092, 27th International Electric Propulsion Conference, Pasadena, CA, Oct. 15–19, 2001.
45. Soulas, G.C., et al., “Performance of Titanium Optics on a NASA 30 cm Ion Thruster,” AIAA–2000–3814, 36th AIAA/ASME/SAE/ASEE Joint Propulsion Conference and Exhibit, Huntsville, AL, Jul. 16–19, 2000.
46. Soulas, G.C., et al., “Performance Evaluation of 40cm Ion Optics for the NEXT Ion Engine,” AIAA–2002–3834, 38th AIAA/ASME/SAE/ASEE Joint Propulsion Conference and Exhibit, Indianapolis, IN, Jul. 7–10, 2002.
47. Van Noord, J.L. and Soulas, G.C., “A Facility and Ion Thruster Back Sputter Survey for Higher Power Ion Thrusters,” AIAA–2005–4067, 41st AIAA/ASME/SAE/ASEE Joint Propulsion Conference and Exhibit, Tucson, AZ, Jul. 10–13, 2005.
48. Christensen, J.A., et al., “Design and Fabrication of a Flight Model 2.3 kW Ion Thruster for the Deep Space 1 Mission,” AIAA–1998–3327, 34th AIAA/ASME/SAE/ASEE Joint Propulsion Conference and Exhibit, 1998.
49. Herman, D.A., et al., “Status of the NEXT Ion Thruster Long-Duration Test after 10,100 h and 207 kg Demonstrated,” AIAA–2007–5272, 43rd AIAA/ASME/SAE/ASEE Joint Propulsion Conference and Exhibit, Cincinnati, OH, Jul. 8–11, 2007.
50. Herman, D.A., et al., “NEXT Long-Duration Test after 11,570 h and 237 kg of Xenon Processed,” IEPC–2007–033, 30th International Electric Propulsion Conference, Florence, Italy, Sep. 17–20, 2007.
51. Sengupta, A., et al., “Status of the Extended Life Test of the Deep Space 1 Flight Spare Ion Engine after 30,352 Hours of Operation,” AIAA–2003–4558, 39th AIAA/ASME/SAE/ASEE Joint Propulsion Conference and Exhibit, Huntsville, AL, Jul. 20–23, 2003.
52. Doerner, R.P. and Goebel, D.M., “Sputtering Yields of Ion Thruster Grid and Cathode Materials during Very Low Xenon Plasma Bombardment,” AIAA–2003–4561, 39th JPC, Huntsville, AL, Jul. 20–23, 2003.

53. Williams, G.J., et al., “Results of the 2000 hr Wear Test of the HiPEP Ion Thruster with Pyrolitic Graphite Ion Optics,” AIAA–2006–4668, 4nnd AIAA/ASME/SAE/ASEE Joint Propulsion Conference and Exhibit, Sacramento, CA, Jul. 9–12, 2006.
54. Britton, M., et al., “Destructive Analysis of the NEXT 2000-Hour Wear Test Hollow Cathode Assemblies,” NASA/TM—2005-213387, NASA Glenn Research Center, Cleveland, OH, Jul. 2005.
55. Malone, S.P. and Soulas, G.C., “Computational Ion Optics Design Evaluations,” AIAA–2004–3784, 40th AIAA/ASME/SAE/ASEE Joint Propulsion Conference and Exhibit, Fort Lauderdale, FL, Jul. 11–14, 2004.
56. Sengupta, A., et al., “Wear Characteristics from the Extended Life Test of the DS1 Flight Spare Ion Thruster,” 28th International Electric Propulsion Conference, Toulousse, France, Mar. 17–21, 2003.
57. Polk, J.E., et al., “The Effect of Carbon Deposition on Accelerator Grid Wear Rates in Ion Engine Ground Testing,” AIAA–2000–3662, 36th AIAA/ASME/SAE/ASEE Joint Propulsion Conference and Exhibit, Huntsville, AL, Jul. 17–19, 2000.
58. Williams, G.J. and Gilland, J.H., “Modeling of the Accelerator Grid Erosion of the NASA Evolutionary Xenon Thruster (NEXT),” IEPC–2007–375, 30th International Electric Propulsion Conference, Florence, Italy, Sep. 17–20, 2007.
59. Anderson, J.R., et al., “Results of an On–going Long Duration Ground Test of the DS1 Flight Spare Ion Engine,” AIAA–1999–2857, 35th AIAA/ASME/SAE/ASEE Joint Propulsion Conference and Exhibit, Los Angeles, CA, Jun. 20–24, 1999.
60. Diaz, E. and Soulas, G.C., “Grid Gap Measurement for an NSTAR Ion Thruster,” IEPC–2005–244, 29th International Electric Propulsion Conference, Princeton, NJ, Oct. 31–Nov. 4, 2005.
61. Snyder, J.S., et al., “Environmental Testing of the NEXT PM1 Ion Engine,” AIAA–2007–5275, 43rd AIAA/ASME/SAE/ASEE Joint Propulsion Conference and Exhibit, Cincinnati, OH, Jul. 8–11, 2007.
62. Van Noord, J.L., “NEXT Ion Thruster Thermal Model,” AIAA–2007–5218, 43rd AIAA/ASME/SAE/ASEE Joint Propulsion Conference and Exhibit, Cincinnati, OH, Jul. 8–11, 2007.
63. Soulas, G.C. and Frandina, M.M., “Ion Engine Grid Gap Measurements,” AIAA–2004–3961, 40th AIAA/ASME/SAE/ASEE Joint Propulsion Conference and Exhibit, Fort Lauderdale, FL, Jul. 11–14, 2004.
64. Polk, J.E., et al., “The Effect of Engine Wear on Performance in the NSTAR 8000 Hour Ion Engine Endurance Test,” AIAA–1997–0869, 33rd AIAA/ASME/SAE/ASEE Joint Propulsion Conference and Exhibit, Seattle, WA, Jul. 6–9, 1997.

REPORT DOCUMENTATION PAGE		Form Approved OMB No. 0704-0188

1. REPORT DATE *(DD-MM-YYYY)*	2. REPORT TYPE	3. DATES COVERED *(From - To)*
01-05-2009	Technical Memorandum	

4. TITLE AND SUBTITLE
NEXT Long-Duration Test Plume and Wear Characteristics After 16,550 h of Operation and 337 kg of Xenon Processed

5a. CONTRACT NUMBER

5b. GRANT NUMBER

5c. PROGRAM ELEMENT NUMBER

6. AUTHOR(S)
Herman, Daniel, A.; Soulas, George, C.; Patterson, Michael, J.

5d. PROJECT NUMBER

5e. TASK NUMBER

5f. WORK UNIT NUMBER
WBS 346620.04.05.03.13

7. PERFORMING ORGANIZATION NAME(S) AND ADDRESS(ES)
National Aeronautics and Space Administration
John H. Glenn Research Center at Lewis Field
Cleveland, Ohio 44135-3191

8. PERFORMING ORGANIZATION REPORT NUMBER
E-16929

9. SPONSORING/MONITORING AGENCY NAME(S) AND ADDRESS(ES)
National Aeronautics and Space Administration
Washington, DC 20546-0001

10. SPONSORING/MONITORS ACRONYM(S)
NASA

11. SPONSORING/MONITORING REPORT NUMBER
NASA/TM-2009-215613; AIAA-2008-4919

12. DISTRIBUTION/AVAILABILITY STATEMENT
Unclassified-Unlimited
Subject Category: 20
Available electronically at http://gltrs.grc.nasa.gov
This publication is available from the NASA Center for AeroSpace Information, 301-621-0390

13. SUPPLEMENTARY NOTES

14. ABSTRACT
The NASA's Evolutionary Xenon Thruster (NEXT) program is developing the next-generation ion propulsion system with significant enhancements beyond the state-of-the-art. The NEXT ion propulsion system provides improved mission capabilities for future NASA science missions to enhance and enable Discovery, New Frontiers, and Flagship-type NASA missions. As part of a comprehensive thruster service life assessment utilizing both testing and analyses, a Long-Duration Test (LDT) was initiated to validate and qualify the NEXT propellant throughput capability to a qualification-level of 450 kg, 1.5 times the mission-derived throughput requirement of 300 kg. This wear test is being conducted with a modified, flight-representative NEXT engineering model ion thruster, designated EM3. As of June 25, 2008, the thruster has accumulated 16,550 h of operation: the first 13,042 h at the thruster full-input-power of 6.9 kW with 3.52 A beam current and 1800 V beam power supply voltage. Operation since 13,042 h, i.e., the most recent 3,508 h, has been at an input power of 4.7 kW with 3.52 A beam current and 1180 V beam power supply voltage. The thruster has processed 337 kg of xenon (Xe) surpassing the NSTAR propellant throughput demonstrated during the extended life testing of the Deep Space 1 flight spare. The NEXT LDT has demonstrated a total impulse of 13.3×106 N·s; the highest total impulse ever demonstrated by an ion thruster. Thruster plume diagnostics and erosion measurements are obtained periodically over the entire NEXT throttle table with input power ranging 0.5 to 6.9 kW. Observed thruster component erosion rates are consistent with predictions and the thruster service life assessment. There have not been any observed anomalous erosion and all erosion estimates indicate a thruster throughput capability that exceeds ~750 kg of Xe, an equivalent of 36,500 h of continuous operation at the full-power operating condition. This paper presents the erosion measurements and plume diagnostic results for the NEXT LDT to date with emphasis on the change in thruster operating condition and resulting impact on wear characteristics. Ion optics' grid-gap data, both cold and operating, are presented. Performance and wear predictions for the LDT throttle profile are presented.

15. SUBJECT TERMS
Ion engines; Ion optics; Ion propulsion; Electric propulsion; Electrostatic propulsion; Plasma propulsion

16. SECURITY CLASSIFICATION OF:			17. LIMITATION OF ABSTRACT	18. NUMBER OF PAGES	19a. NAME OF RESPONSIBLE PERSON
a. REPORT	b. ABSTRACT	c. THIS PAGE			STI Help Desk (email:help@sti.nasa.gov)
U	U	U	UU	36	19b. TELEPHONE NUMBER *(include area code)* 301-621-0390